BULLETIN OF THE POLISH ACADEMY OF SCIENCES
TECHNICAL SCIENCES, Vol. 60, No. 3, 2012
DOI: 10.2478/v10175-012-0065-y

Closed-loop control algorithm for some class of nonholonomic systems using polar representation

D. PAZDERSKI, P. SZULCZYŃSKI, and K. KOZŁOWSKI*

Poznań University of Technology, Chair of Control and Systems Engineering, 3a Piotrowo St., 60-965 Poznań, Poland

Abstract. This paper is focused on the convergence problem defined for some class of a two input affine nonholonomic driftless system with three-dimensional state. The problem is solved based on a polar transformation which is singular at the origin. The convergence is ensured using static-state feedback. The necessary conditions for construction of the algorithm are formally discussed. The solution, in general, is local, and the feasible domain is strictly related to the properties of the control system. In order to improve algorithm robustness a simple hybrid algorithm is formulated. The general theory is illustrated by two particular systems and the results of numerical simulations are provided.

Key words: polar coordinates, nonholonomic system, discontinuous stabilization at the origin.

1. Introduction

Nonholonomic systems, namely the systems with nonintegrable velocity constraints, constitute an important class of dynamic control systems. It is known that they are of great importance in many areas including applications in robotics. According to the well-known Brockett's theorem [1] there is no possibility to use classical static state feedback in order to stabilize them around an equilibrium point. Therefore the control problem is challenging and have attracted many researchers in the field of control theory for almost 30 years.

In general two main control approaches for asymptotic stabilization have been proposed. The first one presented, for example, in [2, 3] takes advantage of time-varying signals in order to introduce persistent excitation to the closed-loop system. The second one relies on non-smooth techniques including non-smooth coordinate transformation (see for example [4–6]) for which Brockett's obstruction no longer exists. However, discontinuous (or even non-smooth) algorithms may not ensure stability in the classical sense (related to the Lyapunov theory) and, in general, they are not robust to some class of disturbances [7, 8]. Discontinuous or even non smooth "stabilizers" are often named as almost stabilizers, because they guarantee convergence to the desired point but not stabilization due to singularity at the point. Such a drawback becomes one of the most important motivation for developing alternative and smooth control approach taking advantage of so-called transverse functions [9].

Another important techniques used to control the nonholonomic systems are related to the open-loop strategies that are focused on trajectory planning in the presence of phase constraints. These algorithms may take advantage of Lie algebra [10, 11], harmonic inputs [12], differential flatness [13], Newton's numerical computation approach [14] and many others.

In this paper we focus on the closed-loop control using non-smooth transformation that takes advantage of the time-invariant feedback. This approach was originally presented by Astolfi [5] to develop asymptotically convergent controller. The other solution was introduced by Aicardi and others [15] to control unicycle-like robots. This proposition is based on a polar representation that has a convenient interpretation with respect to the given kinematics. In [16], where different control algorithms designed for two-wheeled robots were compared experimentally, it is stated that the control in polar coordinates gives possibility to achieve good transient behavior when applied to the parking problem, but it is difficult to extend it to other systems.

In spite of it an extension of this idea was proposed by Pazderski and others for the first-order chained system and the three link nonholonomic manipulator [17, 18]. The main contribution of this paper is the formulation of a control algorithm designed for quite general two input affine driftless systems. For the best authors' knowledge it is the only solution that uses a polar transformation applicable to control such the class of systems presented so far.

The paper is organized as follows. In Section 2 the control system is defined. Section 3 is focused on the non-smooth coordinates polar transformation that gives a non-continuous dynamic system. Next section is devoted to development of the control closed loop-algorithm. Section 5 is dedicated to application of the proposed theory to control selected systems. In order to illustrate the controller performance extensive simulation results are given. Section 6 concludes the paper.

2. Control system description

Consider the following two-input driftless affine system with three dimensional state $\boldsymbol{x} \in \mathcal{X} \subset \mathbb{R}^3$ defined by

$$\Sigma : \quad \dot{\boldsymbol{x}} = \boldsymbol{g}_1(\boldsymbol{x})\, u_1 + \boldsymbol{g}_2(\boldsymbol{x})\, u_2, \tag{1}$$

*e-mail: krysztof.kozlowski@put.poznan.pl

Unauthenticated | 89.67.242.59
Download Date | 5/19/13 8:28 PM

where u_1 and $u_2 \in \mathbb{R}$ denote control inputs, while $\boldsymbol{g}_1(\boldsymbol{x})$ and $\boldsymbol{g}_2(\boldsymbol{x}) \in \mathbb{R}^3$ are basic vector fields given by

$$\boldsymbol{g}_1(\boldsymbol{x}) := [g_{11}(\boldsymbol{x})\ 0\ 0]^\top,\ \boldsymbol{g}_2(\boldsymbol{x}) := \left[g_{21}(\boldsymbol{x})\ \boldsymbol{g}_2^{*\top}(\boldsymbol{x})\right]^\top, \quad (2)$$

with $\boldsymbol{g}_2^*(\boldsymbol{x}) := [g_{22}(\boldsymbol{x})\ g_{23}(\boldsymbol{x})]^\top \in \mathbb{R}^2$ and $g_{(\cdot)}(\boldsymbol{x}) \in \mathbb{R}$ being real-valued functions. It is assumed that these vector fields satisfy the following properties:

A1: $\forall \boldsymbol{x} \in \mathcal{X}\ \ \|\boldsymbol{g}_1(\boldsymbol{x}(t))\|, \|\boldsymbol{g}_2(\boldsymbol{x}(t))\| < \infty$, where $\|\cdot\|$ denotes Euclidean norm of a vector,

A2: $\forall \boldsymbol{x} \in \mathcal{X}\ \boldsymbol{g}_2(\boldsymbol{x}) \in C^\kappa$ with $\kappa = 1, 2, \ldots$, where C^k stands for a space of continuous functions up to the k^{th} derivative inclusive,

A3: $\forall \boldsymbol{x} \in \mathcal{X}\ |g_{11}(\boldsymbol{x})|, \|\boldsymbol{g}_2^*(\boldsymbol{x})\| > M_1 > 0$,where M_1 is a small positive constant,

A4: $\forall \boldsymbol{x} \in \mathcal{X}\ \dfrac{\partial \boldsymbol{g}_2^*}{\partial x_1} \neq \boldsymbol{0}$,

A5: The following algebraic equation

$$\arg\left(\boldsymbol{g}_2^*(\boldsymbol{x}^0)\right) - \arg\left(\boldsymbol{g}_2^*(\boldsymbol{0})\right) = 0, \quad (3)$$

where $\boldsymbol{x}^0 := [x_1\ 0\ 0]^\top \in \mathcal{X}$ and $\arg(\cdot)$ denotes operator defined in Appendix by Eq. (78), is satisfied for unique value of $x_1 = 0$ in the neighborhood of zero.

Assumptions A1 and A2 are needed to ensure that the system and derivative of $\boldsymbol{g}_2$ are well defined $\forall \boldsymbol{x} \in \mathcal{X}$, while assumptions A3 and A4 can be interpreted as necessary conditions for system Σ to be controllable. The last property, A5, comes from the requirement of solution uniqueness and it is explained more carefully in Sec. 4.

3. Discontinuous transformation

Taking advantage of the particular form of the vector field $\boldsymbol{g}_1$ one can easily decompose the system Σ into the following two subsystems:

$$\Sigma_1: \quad \dot{x}_1 = g_{11}(\boldsymbol{x})\,u_1 + g_{21}(\boldsymbol{x})\,u_2, \quad (4)$$

$$\Sigma_2: \quad \dot{\boldsymbol{x}}^* = \boldsymbol{g}_2^*(\boldsymbol{x})\,u_2, \quad (5)$$

where $\boldsymbol{x}^* := [x_2\ x_3]^\top$. Next, using polar representation described in Appendix, one can chose

$$\rho_\alpha := \|\boldsymbol{x}^*\| \quad (6)$$

and

$$\alpha := \arg \boldsymbol{x}^* \quad (7)$$

as the new state variables instead of x_2 and x_3. Taking time derivative of (6), (7) and using (5) the following dynamics can be derived

$$\dot{\rho}_\alpha = \rho_\beta \cos(\beta - \alpha)\,u_2, \quad (8)$$

and

$$\dot{\alpha} = \frac{\rho_\beta}{\rho_\alpha}\sin(\beta - \alpha)\,u_2, \quad (9)$$

where

$$\rho_\beta := \|\boldsymbol{g}_2^*(\boldsymbol{x})\| \quad (10)$$

and

$$\beta := \arg\left(\boldsymbol{g}_2^*(\boldsymbol{x})\right) \in \Omega \quad (11)$$

is the third transformed state. Considering time evolution of β and referring to general result given in Appendix by Eq. (79) one has

$$\dot{\beta} = \frac{1}{\rho_\beta}\boldsymbol{\psi}^\top(\beta)\,\boldsymbol{J}\dot{\boldsymbol{g}}_2^*(\boldsymbol{x}) = \frac{1}{\rho_\beta}\boldsymbol{\psi}^\top(\beta)\,\boldsymbol{J}\frac{\partial \boldsymbol{g}_2^*(\boldsymbol{x})}{\partial \boldsymbol{x}}\dot{\boldsymbol{x}}, \quad (12)$$

where $\boldsymbol{\psi}(\cdot)$ and $\boldsymbol{J}$ are defined in Appendix by Eqs. (75) and (80), respectively. Expanding the last term of Eq. (12) as

$$\frac{\partial \boldsymbol{g}_2^*(\boldsymbol{x})}{\partial \boldsymbol{x}}\dot{\boldsymbol{x}} = \frac{\partial \boldsymbol{g}_2^*(\boldsymbol{x})}{\partial x_1}\dot{x}_1 + \frac{\partial \boldsymbol{g}_2^*(\boldsymbol{x})}{\partial \boldsymbol{x}^*}\dot{\boldsymbol{x}}^*$$

and using relationships (4)-(5) one obtains

$$\begin{aligned}\dot{\beta} &= h_1\left(g_{11}(\boldsymbol{x})u_1 + g_{21}(\boldsymbol{x})u_2\right) + h_2 u_2 \\ &= h_1 g_{11}(\boldsymbol{x})u_1 + \left(h_2 + h_1 g_{21}(\boldsymbol{x})\right)u_2,\end{aligned} \quad (13)$$

where

$$h_1 := \frac{1}{\rho_\beta}\boldsymbol{\psi}^\top(\beta)\,\boldsymbol{J}\frac{\partial \boldsymbol{g}_2^*(\boldsymbol{x})}{\partial x_1}, \quad (14)$$

$$h_2 := \boldsymbol{\psi}^\top(\beta)\,\boldsymbol{J}\frac{\partial \boldsymbol{g}_2^*(\boldsymbol{x})}{\partial \boldsymbol{x}^*}\frac{\boldsymbol{g}_2^*(\boldsymbol{x})}{\rho_\beta} = \boldsymbol{\psi}^\top(\beta)\,\boldsymbol{J}\frac{\partial \boldsymbol{g}_2^*(\boldsymbol{x})}{\partial \boldsymbol{x}^*}\boldsymbol{\psi}(\beta) \quad (15)$$

are auxiliary bounded functions for $\boldsymbol{x} \in \mathcal{X}$ (it is guaranteed by assumptions A1, A2 and A3).

Summarizing, applying change of coordinates given by (6), (7) and (11) and taking into account the definition of the system Σ yields in the following discontinuous system Σ^d:

$$\Sigma_1^d: \ \dot{\rho}_\alpha = \rho_\beta\cos(\beta - \alpha)\,u_2, \quad (16)$$

$$\Sigma_2^d: \ \dot{\alpha} = \frac{\rho_\beta}{\rho_\alpha}\sin(\beta - \alpha)\,u_2, \quad (17)$$

$$\Sigma_3^d: \ \dot{\beta} = h_1 g_{11}(\boldsymbol{x})u_1 + \left(h_2 + h_1 g_{21}(\boldsymbol{x})\right)u_2. \quad (18)$$

From (17) it can be seen that system Σ^d is intrinsically singular at $\rho_\alpha = 0$ as a result of singularity of the polar representation at zero (in that case value of angle α cannot be longer determined). However, for $\rho_\alpha > 0$ the system becomes well-defined if assumptions A1, A2, A3 and A4 are satisfied.

4. Controller design

4.1. Control problem formulation. Now we formally define the control convergence problem investigated in this paper.

Problem 1 [Convergence problem]. Assuming that $\boldsymbol{x}(0) \in \mathcal{X}$ find bounded controls u_1 and u_2 such that for $t > 0$ trajectory $\boldsymbol{x}(t) \in \mathcal{X}$ uniformly converges to zero, namely

$$\lim_{t\to\infty} \boldsymbol{x}(t) = \boldsymbol{0}. \quad (19)$$

This problem is solved taking advantage of system Σ^d which is discontinuous at the origin. As a result we refer to the properties of polar representation given by (6), (7) and (11). It is clear that map $\rho_\alpha : \mathbb{R}^2 \to \mathbb{R}$ is a surjection which preserves the origin, namely

$$(\rho_\alpha = 0) \Rightarrow (\boldsymbol{x}^* = \boldsymbol{0}). \quad (20)$$

Unauthenticated | 89.67.242.59
Download Date | 5/19/13 8:28 PM

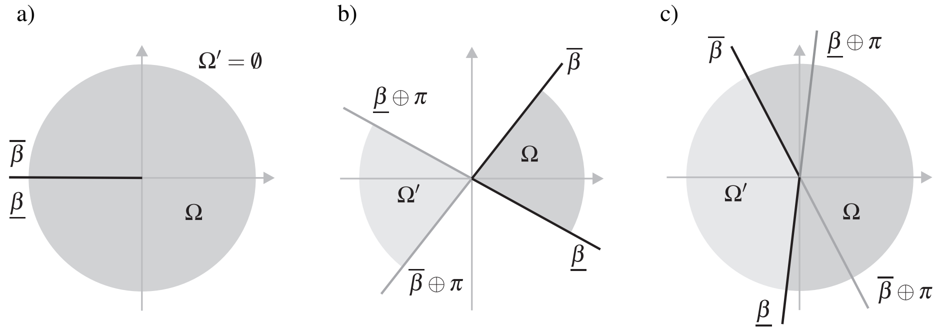

Fig. 1. Illustration of sets Ω and Ω'. Case A: $\Omega = (-\pi, \pi]$, Case B: $\overline{\beta} \ominus \underline{\beta} < \pi$, Case C: $\overline{\beta} \ominus \underline{\beta} \geq \pi$

Moreover, for $\rho_\alpha \equiv 0$ the following definition is considered: $\beta_0 := \arg(\boldsymbol{g}_2^*(\mathbf{0}))$. Then taking into account the assumption A5 at the neighborhood of zero (in order to guarantee uniqueness of the solution) implies that

$$(\beta = \beta_0) \Rightarrow (x_1 = 0). \tag{21}$$

Hence, taking advantage of implications (20) and (21) the original control problem can be redefined with respect to the discontinuous system Σ^d as follows:

$$\lim_{t\to\infty} \rho_\alpha(t) = 0, \qquad \lim_{t\to\infty} \beta(t) = \beta_0. \tag{22}$$

Comparing evolution of α and β one should be aware that Ω is a simply connected subset of $(-\pi, \pi]$. To be more precisely, we define the following open set

$$\Omega := \left\{\beta : \underline{\beta} < \beta < \overline{\beta}\right\} \tag{23}$$

with $\underline{\beta} < \overline{\beta}$ being parameters defining boundary of the set. Additionally, the following auxiliary set is introduced

$$\Omega' := \left\{\beta : \underline{\beta} \oplus \pi < \beta < \overline{\beta} \oplus \pi\right\} - \Omega \subset (-\pi, \pi], \tag{24}$$

where $\oplus$ is the modulo operator described in Appendix. Consequently, one can take into account three particular cases that are illustrated in Fig. 1.

To facilitate the design of the controller we introduce two control subtasks described as follows.

1. Find bounded control input u_2 such that $\rho_\alpha(t), \dot{\rho}_\alpha(t), \dot{\alpha}(t) \in \mathcal{L}_\infty$, where $\mathcal{L}_\infty$ stands for a space of scalar functions of time $f(t) \in \mathbb{R}$ such that $\sup_t |f(t)| < \infty$, with $|\cdot|$ denoting absolute value of scalar function $f(t)$,
2. Assuming that $\alpha(0) \in \Omega \cup \Omega'$ find bounded control input u_1 such that

$$\lim_{t\to\infty} \sin(\beta(t) - \alpha(t)) = 0, \tag{25}$$

and for $\lim_{t\to\infty} \rho_\alpha(t) = 0$

$$\lim_{t\to\infty} \beta(t) = \beta_0. \tag{26}$$

4.2. Control solution. The well-known Brockett's theory [1] which investigates the necessary conditions for asymptotic stabilization using static state feedback is formulated with respect to continuous control systems. Since Σ^d at the origin is not continuous Brockett's theory is not applicable anymore. As a result it is possible to use classic feedback to make an error trajectory convergent to the desired point. The algorithm formulated in this paper is strongly based on this property.

Proposition 1 (First control task). The continuous control law written as

$$u_2 := -k_2 \rho_\beta^{-1} \cos^m(\beta - \alpha) \cdot \rho_\alpha, \tag{27}$$

where $k_2 > 0$ and $m := 2k + 1$ with $k = 0, 1, 2, \ldots$ makes system Σ_1^d stable.

Proof 1. Let us define Lyapunov function candidate as $V_1 := \frac{1}{2}\rho_\alpha^2$. Applying control (27) to system Σ_1^d (16) gives the following closed-loop dynamics

$$\dot{\rho}_\alpha = -k_2 \rho_\alpha \cos^{m+1}(\beta - \alpha). \tag{28}$$

Next, calculating time derivative of V_1 and using (28) yields in

$$\dot{V}_1 = \rho_\alpha \dot{\rho}_\alpha = -k_2 \cos^{m+1}(\beta - \alpha) \cdot \rho_\alpha^2 \leq 0. \tag{29}$$

Since $\dot{V}_1$ is semi-negative definite $\forall t > 0$, $V_1(t) \leq V_1(0)$ and $\forall t > 0$, $\rho_\alpha(t) \leq \rho_\alpha(0)$ thus $\rho_\alpha(t) \in \mathcal{L}_\infty$.

Now we investigate boundedness of the control signals. From $\rho_\alpha(t) \in \mathcal{L}_\infty$ and $\rho_\beta > 0$ (it follows from assumption A3) and Eq. (27) implies that $u_2(t) \in \mathcal{L}_\infty$. Using (27) in (17) allows one to consider the following closed-loop dynamics

$$\dot{\alpha} = -k_2 \sin(\beta - \alpha) \cos^m(\beta - \alpha). \tag{30}$$

Equation (30) implies that $\dot{\alpha}(t) \in \mathcal{L}_\infty$. Taking into account that $\rho_\alpha \in \mathcal{L}_\infty$ it can be concluded from (28) that $\dot{\rho}_\alpha(t) \in \mathcal{L}_\infty$.

Proposition 2 (Second control task). Suppose that there exists a function $\gamma : \Omega \cup \Omega' \times \Omega \to \mathbb{R}$ having the following properties for any $\alpha \in \Omega \cup \Omega'$ and $\beta \in \Omega$:

A6: $\gamma(\alpha, \beta) = 0 \Rightarrow \begin{cases} \alpha = \beta & \text{for } \alpha \in \Omega \\ \alpha = \beta \oplus \pi & \text{for } \alpha \in \Omega' \end{cases}$,

A7: $\left|\dfrac{\partial \gamma(\alpha, \beta)}{\partial \alpha}\right| > M_2 > 0$, $\left|\dfrac{\partial \gamma(\alpha, \beta)}{\partial \beta}\right| > M_3 > 0$,

A8: $\left|\dfrac{\sin(\beta(t) - \alpha(t))}{\gamma(\alpha(t), \beta(t))}\right| < \infty$, $\lim_{\gamma\to 0} \left|\dfrac{\sin(\beta - \alpha)}{\gamma(\alpha, \beta)}\right| > M_4 > 0$,

Unauthenticated | 89.67.242.59
Download Date | 5/19/13 8:28 PM

A9: $\left|\frac{\partial\gamma(\alpha,\beta)}{\partial\alpha}\right|,\left|\frac{\partial\gamma(\alpha,\beta)}{\partial\beta}\right|<\infty,$

A10: $\left|\frac{\partial^2\gamma(\alpha,\beta)}{\partial\alpha^2}\right|,\left|\frac{\partial^2\gamma(\alpha,\beta)}{\partial\alpha\partial\beta}\right|,\left|\frac{\partial^2\gamma(\alpha,\beta)}{\partial\beta^2}\right|<\infty,$

A11: for $\Omega\subset(-\pi,\pi]$ and $\alpha\in\partial\Omega$ $\gamma(\alpha,\beta)=\infty$, where $\partial\Omega$ denotes boundary of the set Ω.

Assuming that $\rho_\alpha(0)>0$ and $\alpha(0)\in\Omega\cup\Omega'$ control law $u_1(t)$ given by

$$\begin{aligned}u_1 := &\frac{1}{h_1 g_{11}}\left(\frac{\partial\gamma(\alpha,\beta)}{\partial\beta}\right)^{-1}\\ &\cdot\Big(-k_1\gamma(\alpha,\beta)+k_2\sin(\beta-\alpha)\cos^m(\beta-\alpha)\frac{\partial\gamma(\alpha,\beta)}{\partial\alpha}\\ &+\frac{k_2}{c}\frac{\sin(\beta-\alpha)}{\gamma(\alpha,\beta)}\gamma(\alpha,\beta_0)\frac{\partial\gamma(\alpha,\beta_0)}{\partial\alpha}\cos^m(\beta-\alpha)\Big)\\ &+\frac{1}{h_1 g_{11}}(h_2+h_1 g_{21})k_2\frac{\rho_\alpha}{\rho_\beta}\cos^m(\beta-\alpha),\end{aligned}\tag{31}$$

where k_1, $c>0$ are design parameters, applied to system Σ^d ensures the boundedness of the control signals and convergence (locally exponential convergence) of α and β according to relationships (25) and (26).

Proof 2. Let

$$V_2 := \frac{1}{2}c\gamma^2(\alpha,\beta)+\frac{1}{2}\gamma^2(\alpha,\beta_0)\tag{32}$$

be a Lyapunov-like function candidate. Taking the time derivative of (32) one can obtain

$$\begin{aligned}\dot V_2 = &c\gamma(\alpha,\beta)\left(\frac{\partial\gamma(\alpha,\beta)}{\partial\alpha}\dot\alpha+\frac{\partial\gamma(\alpha,\beta)}{\partial\beta}\dot\beta\right)\\ &+\gamma(\alpha,\beta_0)\frac{\partial\gamma(\alpha,\beta_0)}{\partial\alpha}\dot\alpha.\end{aligned}\tag{33}$$

Next, substituting the control signals u_1 and u_2 given by (31) and (27) into (18) gives

$$\begin{aligned}\dot\beta = &(-k_1\gamma(\alpha,\beta)+k_2\sin(\beta-\alpha)\cos^m(\beta-\alpha)\\ &\cdot\frac{\partial\gamma(\alpha,\beta)}{\partial\alpha}+\frac{k_2}{c}\frac{\sin(\beta-\alpha)}{\gamma(\alpha,\beta)}\gamma(\alpha,\beta_0)\\ &\cdot\frac{\partial\gamma(\alpha,\beta_0)}{\partial\alpha}\cos^m(\beta-\alpha)\Big)\left(\frac{\partial\gamma(\alpha,\beta)}{\partial\beta}\right)^{-1}.\end{aligned}\tag{34}$$

Using (30) and (34) in (33) yields in

$$\dot V_2 = -ck_1\gamma^2(\alpha,\beta).\tag{35}$$

Taking into account (35) it is clear that $\dot V_2$ is negative semidefinite, hence $V_2(t)\in\mathcal{L}_\infty$. As a result one has

$$\gamma(\alpha(t),\beta(t))\in\mathcal{L}_\infty.\tag{36}$$

Referring to assumption A11 implies that $\alpha\in\Omega\cup\Omega'$, namely α cannot escape from the set Ω or Ω' during convergence process (in opposite case $\gamma(\alpha,\beta)$ would become unbounded and it is a contradiction). It implies that $(\alpha(0)\in\Omega)\Rightarrow(\forall t>0\ \alpha(t)\in\Omega)$ or $(\alpha(0)\in\Omega')\Rightarrow(\forall t>0\ \alpha(t)\in\Omega')$.

In order to show that γ asymptotically converges to zero uniformly boundedness of $\dot V_2$ has to be verified. The time derivative of $\dot V_2$ is calculated as follows

$$\ddot V_2 = -2ck_1\gamma(\alpha,\beta)\left(\frac{\partial\gamma(\alpha,\beta)}{\partial\alpha}\dot\alpha+\frac{\partial\gamma(\alpha,\beta)}{\partial\beta}\dot\beta\right).\tag{37}$$

The boundedness of $\dot\alpha$ was shown in the proof of the Proposition 1. Considering result (36), assumptions A8 and A9 it can be concluded from (34) that $\dot\beta(t)\in\mathcal{L}_\infty$. Consequently it can be shown that $\ddot V_2$ is bounded which implies that $\dot V_2$ is uniformly bounded. Referring to the Barbalat's lemma [19] one can write that

$$\lim_{t\to\infty}\gamma(\alpha(t),\beta(t))=0.\tag{38}$$

Then, taking into account assumption A8 it implies that relationship (25) is satisfied.

The boundedness of control input u_1 can be proved based on (31). Considering that $\rho_\beta>0$, using assumption A1 ($\rho_\beta(t)\in\mathcal{L}_\infty$) and noticing that $h_1(t),h_2(t)\in\mathcal{L}_\infty$ gives directly that $u_1(t)\in\mathcal{L}_\infty$.

Next we investigate the limit of $\dot\beta$ utilizing the Barbalat's lemma once again. In order to simplify the calculations Eq. (34) is rewritten using (28) as follows

$$\begin{aligned}\dot\beta = &\left(-k_1\gamma(\alpha,\beta)-\dot\alpha\frac{\partial\gamma(\alpha,\beta)}{\partial\alpha}-\frac{\dot\alpha}{c}\frac{\gamma(\alpha,\beta_0)}{\gamma(\alpha,\beta)}\frac{\partial\gamma(\alpha,\beta_0)}{\partial\alpha}\right)\\ &\cdot\left(\frac{\partial\gamma(\alpha,\beta)}{\partial\beta}\right)^{-1}.\end{aligned}\tag{39}$$

Then calculating second order time derivative of β one has

$$\begin{aligned}\ddot\beta = &\Big(-k_1\gamma(\alpha,\beta)\left(\frac{\partial\gamma(\alpha,\beta)}{\partial\alpha}\dot\alpha+\frac{\partial\gamma(\alpha,\beta)}{\partial\beta}\dot\beta\right)\\ &-\ddot\alpha\frac{\partial\gamma(\alpha,\beta)}{\partial\alpha}-\dot\alpha\left(\frac{\partial^2\gamma(\alpha,\beta)}{\partial\alpha^2}\dot\alpha+\frac{\partial^2\gamma(\alpha,\beta)}{\partial\alpha\partial\beta}\dot\beta\right)\\ &-\frac{\ddot\alpha}{c}\frac{\gamma(\alpha,\beta_0)}{\gamma(\alpha,\beta)}\frac{\partial\gamma(\alpha,\beta_0)}{\partial\alpha}-\frac{\dot\alpha}{c\gamma(\alpha,\beta)}\frac{\partial\gamma(\alpha,\beta_0)}{\partial\alpha}\\ &\cdot\left(\frac{\partial\gamma(\alpha,\beta_0)}{\partial\alpha}\dot\alpha-\left(\frac{\partial\gamma(\alpha,\beta)}{\partial\alpha}\dot\alpha+\frac{\partial\gamma(\alpha,\beta)}{\partial\beta}\dot\beta\right)\frac{\gamma(\alpha,\beta_0)}{\gamma(\alpha,\beta)}\right)\\ &-\frac{\dot\alpha}{c}\frac{\gamma(\alpha,\beta_0)}{\gamma(\alpha,\beta)}\frac{\partial^2\gamma(\alpha,\beta_0)}{\partial\alpha^2}\dot\alpha\Big)\left(\frac{\partial\gamma(\alpha,\beta)}{\partial\beta}\right)^{-1}\\ &-\left(\frac{\partial^2\gamma(\alpha,\beta)}{\partial\alpha\partial\beta}\dot\alpha+\frac{\partial^2\gamma(\alpha,\beta)}{\partial^2\beta}\dot\beta\right)\\ &\cdot\left(k_1\gamma(\alpha,\beta)+\frac{\partial\gamma(\alpha,\beta)}{\partial\alpha}\dot\alpha+\frac{\dot\alpha}{c}\frac{\gamma(\alpha,\beta_0)}{\gamma(\alpha,\beta)}\frac{\partial\gamma(\alpha,\beta_0)}{\partial\alpha}\right)\\ &\cdot\left(\frac{\partial\gamma(\alpha,\beta)}{\partial\beta}\right)^{-2}.\end{aligned}\tag{40}$$

Now we consider the boundedness of each term of Eq. (40). Taking the time derivative of $\dot\alpha$ leads to

$$\begin{aligned}\ddot\alpha = &k_2(\dot\beta-\dot\alpha)\left(-\cos^{m+1}(\beta-\alpha)\right.\\ &\left.+m\sin^2(\beta-\alpha)\cos^{m-1}(\beta-\alpha)\right).\end{aligned}\tag{41}$$

Since $\dot\alpha$, $\dot\beta\in\mathcal{L}_\infty$ one can easily show that $\ddot\alpha(t)\in\mathcal{L}_\infty$. Next, taking into account (30), (41) and utilizing assumption

Unauthenticated | 89.67.242.59
Download Date | 5/19/13 8:28 PM

A8 it can be proved that the terms $\dot{\alpha}/\gamma(\alpha,\beta)$ and $\ddot{\alpha}/\gamma(\alpha,\beta)$ remain bounded. Noticing that norm of the first and second order derivatives of γ are bounded and $\frac{\partial\gamma}{\partial\beta} \neq 0$ (cf. assumptions A7, A9 and A10) it can be proved that each term in Eq. (40) is bounded. As a consequence one has $\ddot{\beta}(t) \in \mathcal{L}_\infty$. Considering that $\dot{\beta}$ is uniformly bounded and

$$\left|\int_0^\infty \dot{\beta}(t)\,dt\right| = \left|\lim_{t\to\infty}\beta(t) - \beta(0)\right| < \infty$$

from the Barballat's lemma it follows that

$$\lim_{t\to\infty}\dot{\beta}(t) = 0. \tag{42}$$

Using (42) in (34) one has

$$\lim_{t\to\infty}\Bigg(-k_1\gamma(\alpha(t),\beta(t)) + k_2\sin(\beta(t)-\alpha(t))\cos^m(\beta(t) -\alpha(t))\frac{\partial\gamma(\alpha(t),\beta(t))}{\partial\alpha(t)} + \frac{k_2}{c}\frac{\sin(\beta(t)-\alpha(t))}{\gamma(\alpha(t),\beta(t))} \cdot\gamma(\alpha(t),\beta_0)\frac{\partial\gamma(\alpha(t),\beta_0)}{\partial\alpha(t)}\cos^m(\beta(t)-\alpha(t))\Bigg) \cdot\left(\frac{\partial\gamma(\alpha,\beta)}{\partial\beta}\right)^{-1} = 0. \tag{43}$$

Taking advantage of (38), (25) and assumption A7 one can prove that the only solution of Eq. (43) is $\lim_{t\to\infty}\gamma(\alpha(t),\beta_0) = 0$. Since $\lim_{t\to\infty}\gamma(\alpha(t),\beta(t)) = \gamma(\alpha,\beta_0) = 0$ utilizing assumption A6 one can conclude that relationship (26) is satisfied.

Asymptotic convergence proved here does not give any insight on the convergence rate. In order to describe the controller performance locally one can consider linear approximation of the closed loop dynamics (30) and (34) in some neighborhood of the desired point. Without lack of generality it is assumed that $\alpha,\beta \in \Omega$ which in view of (25) and (26) implies that α and β converges to β_0. Referring to calculations given in Appendix and relationships (82) and (93) the following linear approximation near point such that $\alpha = \beta_0$ and $\beta = \beta_0$ can be taken into account:

$$\begin{bmatrix}\dot{\tilde{\alpha}}\\ \dot{\tilde{\beta}}\end{bmatrix} = \underbrace{\begin{bmatrix} k_2 & -k_2\\ k_1 + k_2\left(1+\frac{1}{c}\right) & -k_1-k_2\end{bmatrix}}_{=:\boldsymbol{H}}\begin{bmatrix}\tilde{\alpha}\\ \tilde{\beta}\end{bmatrix}. \tag{44}$$

It can be easily found that matrix $\boldsymbol{H}$ is Hurwitz-stable for any k_1, k_2 and $c > 0$. As a result local convergence is exponential. Moreover, calculating the characteristic polynomial of matrix $\boldsymbol{H}$ gives

$$\lambda^2 + k_1\lambda + \frac{k_2^2}{c} = 0, \tag{45}$$

where $\lambda \in \mathbb{C}$ is a complex variable. Next, taking into account the characteristic equation of second order linear system it follows that

$$\omega_0 = \frac{k_2}{\sqrt{c}}, \qquad \zeta = \frac{k_1\sqrt{c}}{2k_2}, \tag{46}$$

where ω_0 and ζ denote frequency of undamped oscillation and damping coefficient, respectively. This result gives possibility to tune the algorithm (by selection of gains k_1, k_2 and parameter c) in order to obtain local desired behavior of the closed-loop dynamics.

Now we formulate the following final proposition.

Proposition 3 (First and second control tasks). Assuming that $\boldsymbol{x}(0) \in \mathcal{X}$ and applying control law defined by Eqs. (31) and (27) to system Σ makes trajectory $\boldsymbol{x}(t)$ asymptotically converge to zero, namely

$$\lim_{t\to\infty}\boldsymbol{x}(t) = \boldsymbol{0}. \tag{47}$$

Proof 3. Here we rely on proofs of the Propositions 1 and 2. The convergence result given by (38) implies that $\lim_{t\to\infty}|\cos(\beta(t) - \alpha(t))| = 1$. Hence, there exists such time instant $\tau > 0$ that $\forall t > \tau\ \cos(\beta(t) - \alpha(t)) \neq 0$. Then one can state that $\forall t > \tau,\ \forall\rho_\alpha(t) > 0,\ \dot{V}_1 < 0$. Therefore for $t > \tau$ function $\dot{V}_1$ becomes a negative definite quadratic form and ρ_α asymptotically converges to zero, namely $\lim_{t\to\infty}\rho_\alpha(t) = 0$. Summarizing, since ρ_α and β asymptotically tend to unique constant values, namely $\rho_\alpha \to 0$, $\beta \to \beta_0$, from the properties of polar representation in view of discussion given in section 4.1 relationship (47) is proved.

Referring to the controller design it is important to emphasize that convergence problem is solved only locally, assuming that initial state $\boldsymbol{x}(0) \in \mathcal{X}$ and the following properties are satisfied:

$$\rho_\alpha(0) > 0 \quad\text{and}\quad \alpha(0) \in \Omega\cup\Omega'. \tag{48}$$

It turns out that feasible set $\mathcal{X}$ is strictly related to properties of vector field $\boldsymbol{g}_2$ of system Σ which determines the set Ω. Therefore if $\boldsymbol{x}(0) \notin \mathcal{X}$ one should first bring $\boldsymbol{x}$ to feasible set $\mathcal{X}$ using for example any open-loop control strategy. This problem is not discussed in this paper and it is assumed that $\boldsymbol{x}(0) \in \mathcal{X}$.

The controller proposed here does not ensure stabilization since it is well defined only for $\rho_\alpha > 0$. At $\boldsymbol{x}^* = 0$ the control law becomes singular that is a clear drawback of the proposed non-smooth map. Theoretically for $\boldsymbol{x}^*(0) \neq \boldsymbol{0}$ such that $\boldsymbol{x}(0) \in \mathcal{X}$ singular point is not achieved in finite time. However, in practice, this problem can be always met. This issue becomes even more critical if uncertainty of state determination is taken into account. In order to improve robustness of the given controller requirement of asymptotic convergence can be relaxed. Here we use simple solution based on switching technique.

Proposition 4 (Robust algorithm). Assuming that $\rho_\alpha \geq \epsilon$, where ϵ is arbitrary chosen constant use control solution given in Proposition 4.2. For $\rho_\alpha \leq \epsilon$ redefine control inputs as follows

$$u_1 := -\frac{k_1}{g_{11}}x_1,\ u_2 := 0. \tag{49}$$

Then trajectory $\boldsymbol{x}$ converges to the neighborhood of zero in the sense given by

$$\lim_{t\to\infty}\|\boldsymbol{x}^*(t)\| \leq \epsilon, \tag{50}$$

Unauthenticated | 89.67.242.59
Download Date | 5/19/13 8:28 PM

$$\lim_{t\to\infty} x_1(t) = 0. \tag{51}$$

Proof 4. Assuming that $\rho_\alpha \geq \epsilon$ the algorithm defined by Proposition 3 implies that ρ_α converges to the given neighborhood of zero. Next, inside the neighborhood, namely for $\rho_\alpha < \epsilon$, the applied control input becomes $u_2 := 0$. Consequently it implies that $\dot{\rho}_\alpha = 0$ and ρ_α cannot go out from the neighborhood. Then the closed-loop dynamics of system Σ_1 becomes: $\dot{x}_1 = -k_1 x_1$ and it is clear that for any $k_1 > 0$ the system is asymptotically (exponentially) stable and trajectory $x_1(t)$ satisfies (51).

In order to increase robustness of the controller even more and to avoid chattering phenomena instead of simple switching one may take advantage of hysteresis. The other possibility is to define the feedback control law u_2 also for $\rho_\alpha < \epsilon$. This solution has been effectively used in [20] for particular examples of control systems.

5. Examples of applications

In this section we illustrate the derived theory applying it to control systems given by

$$\Sigma^A: \quad \dot{\boldsymbol{\xi}} = \begin{bmatrix}1\\0\\0\end{bmatrix} u_1 + \begin{bmatrix}0\\1\\\xi_1\end{bmatrix} u_2 \tag{52}$$

and

$$\Sigma^B: \quad \dot{\boldsymbol{\xi}} = \begin{bmatrix}1\\0\\0\end{bmatrix} u_1 + \begin{bmatrix}0\\1\\\xi_1^2\end{bmatrix} u_2, \tag{53}$$

where $\boldsymbol{\xi} := [\xi_1\ \xi_2\ \xi_3]^\top \in \mathbb{R}^3$. We assume that $\boldsymbol{\xi}_d := [\xi_{d1}\ \xi_{d2}\ \xi_{d3}]^\top \in \mathbb{R}^3$ denotes the desired state. Referring to general form given by Eq. (1) the following term

$$\boldsymbol{x} := \boldsymbol{\xi} - \boldsymbol{\xi}_d \tag{54}$$

is considered as the state (configuration) error.

5.1. System A. System Σ^A is commonly known as the first order chained system [9]. Taking advantage of the coordinate and input transformations some nonholonomic mechanical systems such as unicycle, hoping robot and three link manipulator with nonholonomic gears can be transformed to it [9, 12, 20].

It can be verified that the system satisfies LARC (Lie Algebra Rank Condition) [9] at any point $\boldsymbol{\xi} \in \mathbb{R}^3$, hence it is globally small-time controllable. It is worth to notice that LARC is ensured taking into account two layers of the control Lie algebra (including the first order Lie bracket).

Taking advantage of the change of coordinates given by (54) and referring to notation used in Eq. (1) the vector fields become

$$\boldsymbol{g}_1 := [1\ 0\ 0]^\top \text{ and } \boldsymbol{g}_2 := [0\ 1\ (x_1 + \xi_{d1})]^\top. \tag{55}$$

One can easily verify that for these vector fields assumptions A1-A4 are satisfied. Next, using the polar transformation one can obtain the discontinuous system Σ^d defined by Eqs. (16)-(18) with:

$$\begin{aligned}\beta &= \arctan(x_1 + \xi_{d1}), \\ \rho_\beta &= \sqrt{1 + (x_1 + \xi_{d1})^2} = \cos^{-1}(\beta)\end{aligned} \tag{56}$$

and

$$h_1 = \frac{1}{\rho_\beta}[\cos\beta\ \sin\beta]\,\boldsymbol{J}\begin{bmatrix}0\\1\end{bmatrix} = \frac{1}{\rho_\beta}\cos\beta = \cos^2\beta, \tag{57}$$

$$h_2 = 0. \tag{58}$$

The set Ω defined by Eq. (23) is given by:

$$\Omega := \left(-\frac{\pi}{2}, \frac{\pi}{2}\right). \tag{59}$$

Consequently it follows that $\Omega \cup \Omega' = (-\pi, \pi] - \left\{-\frac{\pi}{2}, \frac{\pi}{2}\right\}$. From assumption A5 one has $\arg \boldsymbol{g}_2^*(\boldsymbol{x}^0) = \beta(x_1) = \arctan(x_1 + \xi_{d1})$. Then the following equation has to be considered:

$$\arctan(x_1 + \xi_{d1}) - \beta_0 = 0 \tag{60}$$

with $\beta_0 := \arctan \xi_{d1}$. The only solution of Eq. (60) is $x_1 = 0$.

In order to design the controller it is important to select function γ properly to meet assumptions A8-A12. Here we assume that

$$\gamma(\alpha, \beta) := \tan\beta - \tan\alpha = \frac{\sin(\beta - \alpha)}{\cos\alpha\cos\beta}. \tag{61}$$

It can be verified that conditions A8-A12 are satisfied for $\alpha \in \Omega \cup \Omega'$ and $\beta \in \Omega$.

Referring to the control law given by Eqs. (31) and (27) and considering Eqs. (57), (58) one can calculate

$$\begin{aligned} u_1 = &-k_1\gamma(\alpha,\beta) - k_2\frac{\cos^m(\beta - \alpha)}{\cos^2\alpha} \\ &\cdot\left(\sin(\beta - \alpha) + \frac{1}{c}\cos\alpha\cos\beta\gamma(\alpha, \beta_0)\right),\end{aligned} \tag{62}$$

$$u_2 = -k_2\cos\beta\cos^m(\beta - \alpha)\cdot\rho_\alpha. \tag{63}$$

It is important to note that initial conditions such that $x_2(0) = 0$ is excluded since it implies that $\alpha(0) = \pm\frac{\pi}{2} \notin \Omega \cup \Omega'$.

5.2. System B. System Σ^B can be seen as some variation of the first order chained system. However, its structural properties makes the control problem to be more demanding. In particular, nonholonomy degree of this system is not constant [21]. It can be checked that the LARC condition is satisfied at any point $\boldsymbol{\xi} \in \mathbb{R}^3$ different from zero taking into account two layers of the vector fields generated by the control Lie algebra. However, at $\boldsymbol{\xi} = \boldsymbol{0}$, in order to satisfy the LARC condition, the second order Lie bracket must be taken into account.

Using translation of coordinates given by (54) the vector fields of system Σ^B becomes (cf. definition 1)

$$\boldsymbol{g}_1 := [1\ 0\ 0]^\top \text{ and } \boldsymbol{g}_2 := \left[0\ 1\ (x_1 + \xi_{d1})^2\right]^\top. \tag{64}$$

Unauthenticated | 89.67.242.59
Download Date | 5/19/13 8:28 PM

It is easy to verify that these vector fields satisfy assumptions A1-A4. Taking advantage of the polar transformation one can obtain the discontinuous system Σ^d (see Eqs. (16)-(18) with

$$\beta = \arctan (x_1 + \xi_{d1})^2, \quad \rho_\beta = \sqrt{1 + (x_1 + \xi_{d1})^4} = \cos^{-1}\beta \tag{65}$$

and

$$h_1 = \frac{1}{\rho_\beta}[\cos\beta \ \sin\beta]\, \boldsymbol{J} \begin{bmatrix} 0 \\ 2(x_1 + \xi_{d1}) \end{bmatrix} = 2\cos^2\beta\sqrt{\tan\beta} \tag{66}$$

$$h_2 = 0. \tag{67}$$

The set Ω (see Eq. 23) is defined by

$$\Omega := \left(0, \frac{\pi}{2}\right). \tag{68}$$

As a result one has $\Omega \cup \Omega' = \left(-\pi, -\frac{\pi}{2}\right) \cup \left(0, \frac{\pi}{2}\right)$. Taking into account assumption A5 one has $\arg \boldsymbol{g}_2^* (\boldsymbol{x}^0) = \beta(x_1) = \arctan (x_1 + \xi_{d1})^2$. Then the following equation can be considered

$$\arctan (x_1 + \xi_{d1})^2 - \beta_0 = 0 \tag{69}$$

with $\beta_0 := \arctan \xi_{d1}^2$. Equation (69) is satisfied for $x_1 \in \{0, -2\xi_d\}$ which implies that the solution is not unique. We investigate this problem in sequel. From definition (68) one has conclude that $\beta \in \Omega \Leftrightarrow \forall t \geq 0 \ \ (x_1(t) + \xi_{d1}) \neq 0$. In order to meet this requirement initial value of $x_1(0)$ has to satisfy the following relationship

$$\operatorname{sgn}(x_1(0) + \xi_{d1}) = \operatorname{sgn}\xi_{d1}, \tag{70}$$

where $\operatorname{sgn}(\cdot)$ stands for the *signum function*. Then, it can be shown that x_1 satisfying (70) cannot achieve the value $-2\xi_{d1}$ since it implies that $x_1(t) + \xi_{d1}$ would become zero at some time instant that leads to a contradiction.

In order to design the controller it is important to select the function γ to meet assumptions A8-A12. Here we assume that

$$\gamma(\alpha, \beta) := \cot(2\beta) - \cot(2\alpha) = -2\frac{\sin(\beta - \alpha)\cos(\beta - \alpha)}{\sin 2\beta \sin 2\alpha}. \tag{71}$$

It can be verified that it satisfies assumptions A8-A12.

Referring to control law given by Eqs. (31) and (27) in the considered case and using Eqs. (66) and (67) one can write

$$u_1 = -\frac{\sin^2\beta}{\sqrt{\tan\beta}}\left(-k_1\gamma(\alpha,\beta) + 2k_2\frac{\sin(\beta-\alpha)\cos^m(\beta-\alpha)}{\sin^2 2\alpha}\left(1 + \frac{1}{c}\frac{\gamma(\alpha,\beta_0)}{\gamma(\alpha,\beta)}\right)\right), \tag{72}$$

$$u_2 = -k_2\cos\beta\cos^m(\beta-\alpha)\cdot\rho_\alpha. \tag{73}$$

Taking into account relationship (72) one can notice that initial error $\boldsymbol{x}(0)$ is significantly restricted. In particular the control signal u_1 is not defined for $\tan\beta < 0$, $\beta = 0$ and $\beta \neq \pm\pi/2$ as well as $\sin 2\alpha = 0$.

5.3. Simulation results. In order to verify the proposed control law extensive simulations in Matlab/Simulink environment have been conducted with respect to systems Σ^A and Σ^B. To facilitate the description simulation experiments for systems A and B are denoted by Sim A and Sim B, respectively.

For the first series of simulation experiments the controller parameters (cf. Eqs. (62), (63), (72) and (73)) have been selected as follows: $k_1 = 3$, $k_2 = 1$, $m = 3$ and $c = 0.5$ while the desired configuration has been set as $\boldsymbol{\xi}_d = [3\ 2\ 4]^\top$. The initial conditions have been chosen according to the following list:

- Sim A1 and B1: $\boldsymbol{\xi}(0) = [1\ 4\ 6]^\top$,
- Sim A2 and B2: $\boldsymbol{\xi}(0) = [1\ -1\ 2]^\top$.

Consequently, it can be easily verified that for Sim A1 and B1 $\alpha(0) \in \Omega$, while for Sim A2 and B2 $\alpha(0) \in \Omega'$. Moreover, it can be shown that $\xi_1(0)$ satisfies the requirement given by (69) with respect to system Σ^B.

The results of experiments Sim A1 and Sim B1 are illustrated in Figs. 2 and 3, respectively. Taking into account Figs. 2a, 2b, 3a and 3b one can observe that errors converge to zero asymptotically and trajectory $\boldsymbol{\xi}(t)$ approaches the desired point $\boldsymbol{\xi}_d$ (the solution is unique). The control inputs presented in Figs. 2c and 3c remain bounded and converge to zero. It is worth to point out that the control signals do not show oscillatory behavior. Based on Figs. 2d and 3d one can observe that the functions $\alpha(t)$ and $\beta(t)$ for $t \geq 0$ are in the set Ω and converge to the unique point given by $\beta_0 \in \Omega$.

The results of simulations Sim A2 and B2 are presented in Figs. 4 and 5. In general, the description of these results correspond to the previous case, namely errors converge to zero asymptotically and the control problem is designed correctly. The main difference is related to the evolution of the functions $\alpha(t)$ and $\beta(t)$. From Figs. 4d and 5d it can be seen that for $t \geq 0$ $\alpha(t) \in \Omega'$ while $\beta(t) \in \Omega$ which implies that $\alpha(t)$ and $\beta(t)$ converge to the different points such that $\lim_{t\to\infty}(\alpha(t) \ominus \beta(t)) = \pm\pi$. This observation clearly corresponds to the theoretical considerations. A graphic interpretation of the paths in the configuration space for Sim A1, A2, B1 and B2 is given in Fig. 6. It can be seen that for the selected parameters no oscillatory behavior is observed independent on the initial conditions and the curvature of the paths is clearly bounded.

Next we consider the controller performance with respect to the change of parameters m and c.

The conditions of simulation Sim A3 are the same as for Sim A1, however the parameter m has been changed to $m = 1$ or $m = 9$. From Figs. 7 and 8 it can be seen that for the higher value of m the convergence time increases slightly but the parameter does not influence the transient states considerably. As a result value of m is not critical (typically $m = 1$). However, analyzing the path given in Fig. 11a one can say that for higher m the path becomes more smooth (in the sense that the curvature becomes less).

Unauthenticated | 89.67.242.59
Download Date | 5/19/13 8:28 PM

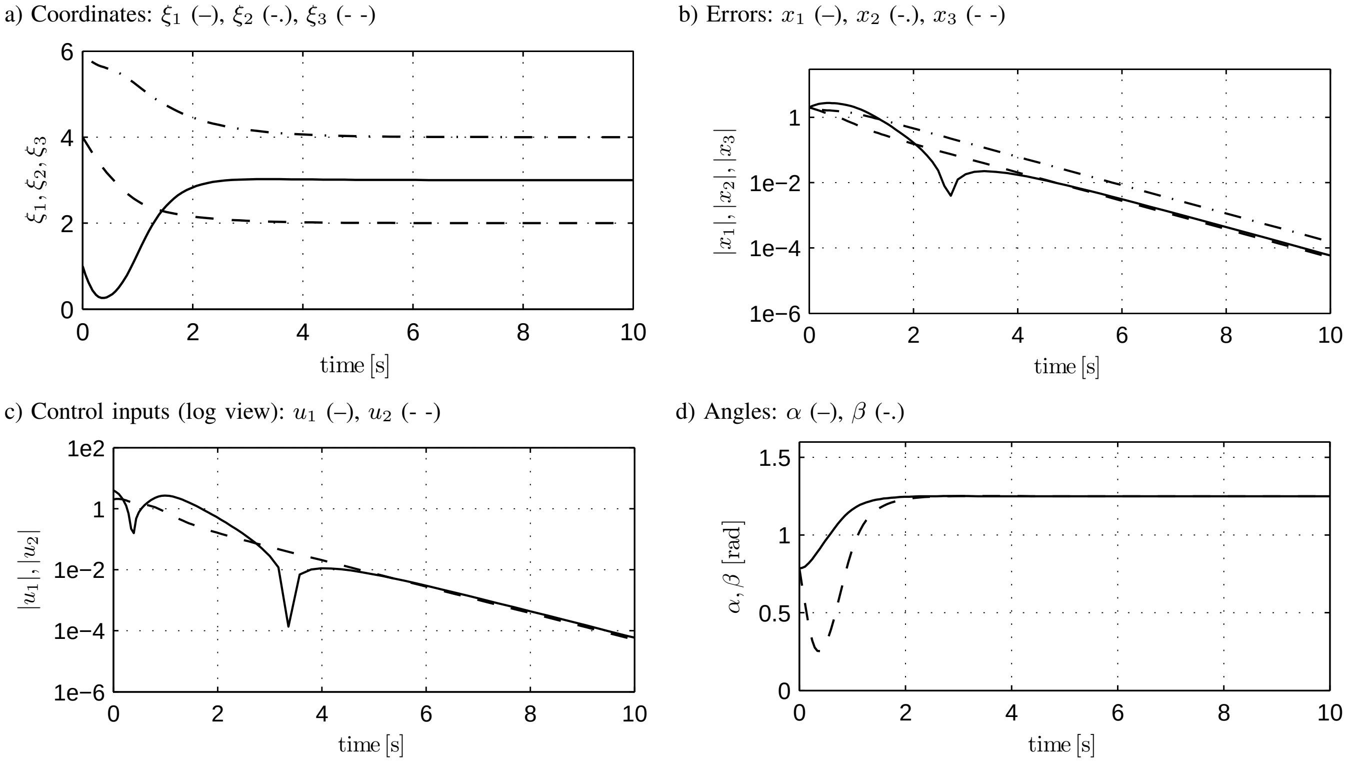

Fig. 2. Results of simulation Sim A1

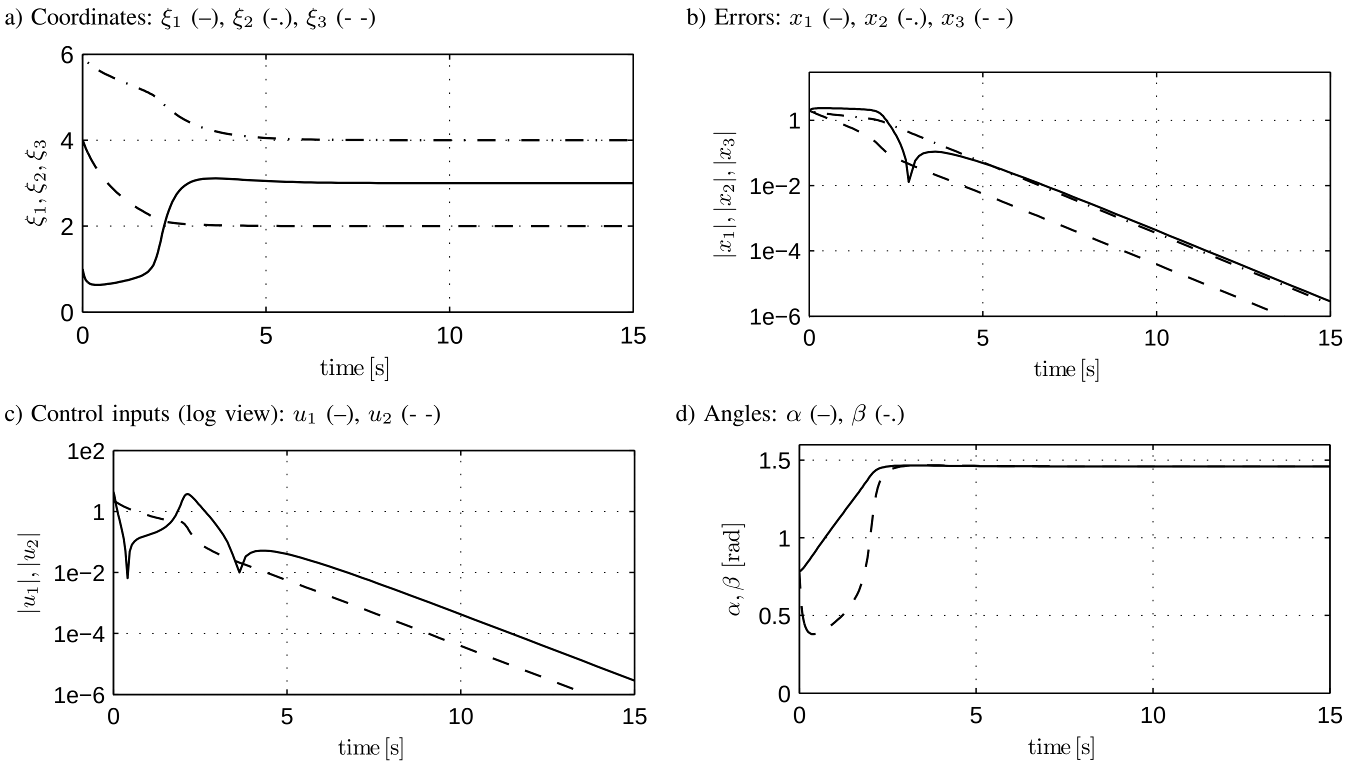

Fig. 3. Results of simulation Sim B1

Unauthenticated | 89.67.242.59
Download Date | 5/19/13 8:28 PM

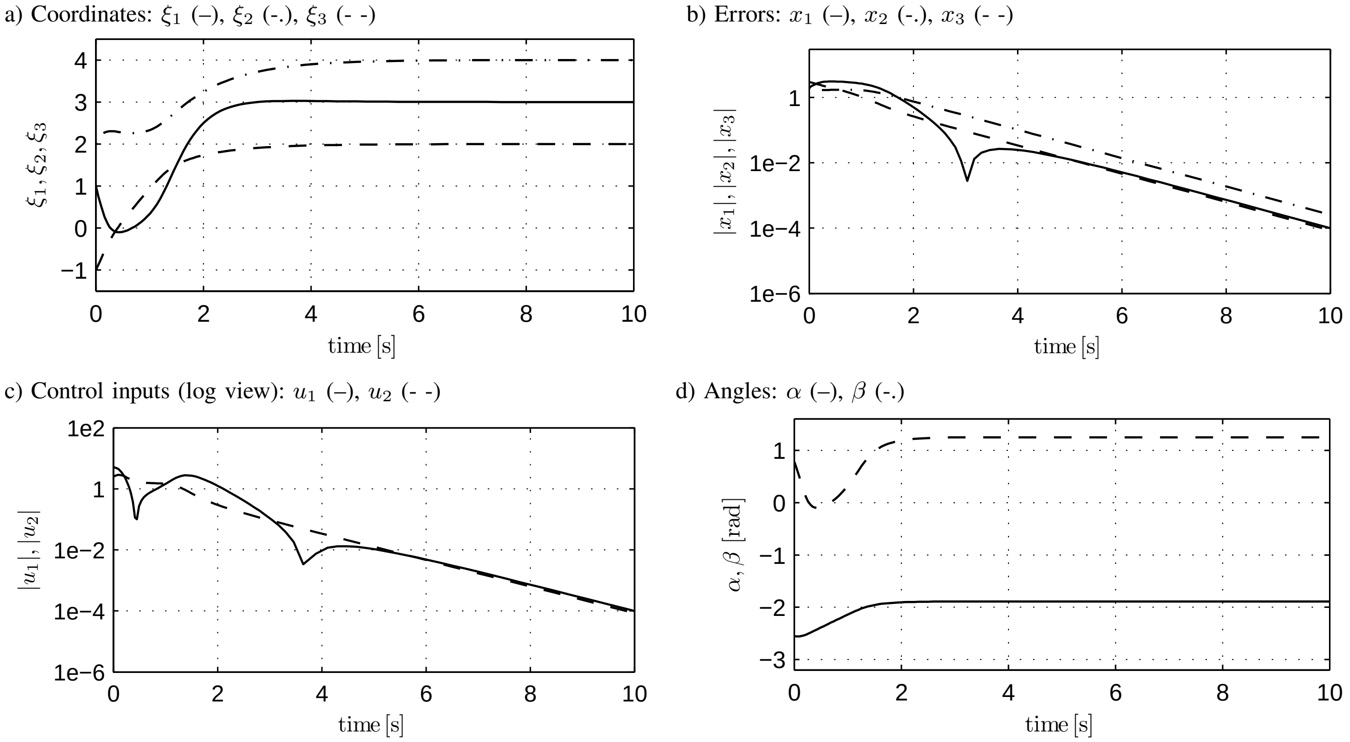

Fig. 4. Results of simulation Sim A2

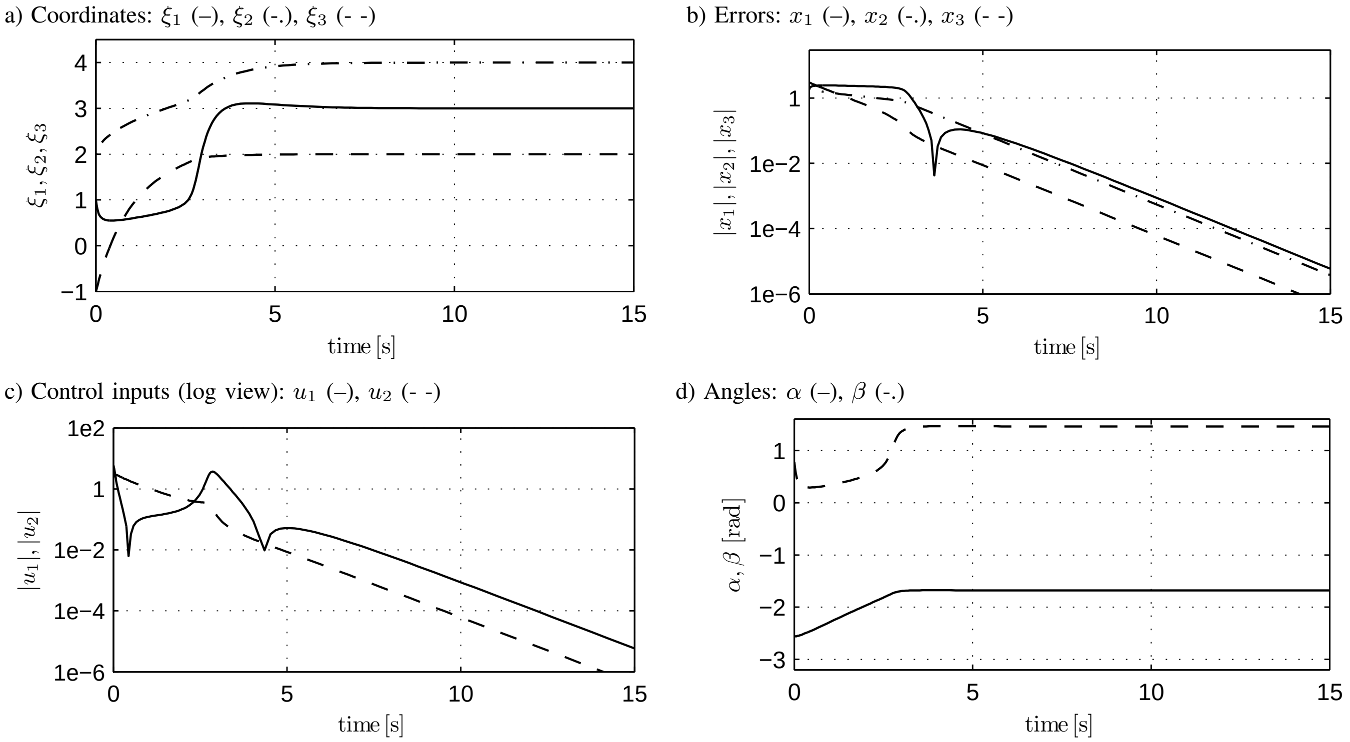

Fig. 5. Results of simulation Sim B2

Unauthenticated | 89.67.242.59
Download Date | 5/19/13 8:28 PM

a) Sim A1 (black line) and A2 (gray line) b) Sim B1 (black line) and B2 (gray line)

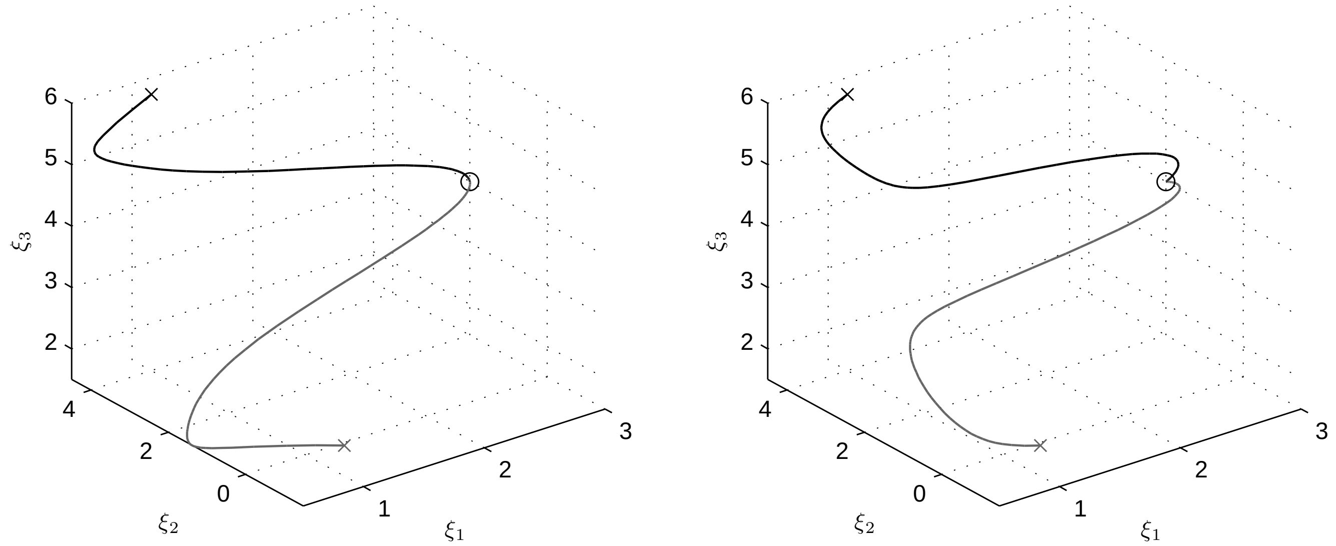

Fig. 6. Path $\boldsymbol{\xi}$ in the coordinate space for simulations Sim A1, A2, B1 and B2: $'\times'$ – initial point, $'\circ'$ – desired point

a) Coordinates: ξ_1 (–), ξ_2 (-.), ξ_3 (- -) b) Angles: α (–), β (-.)

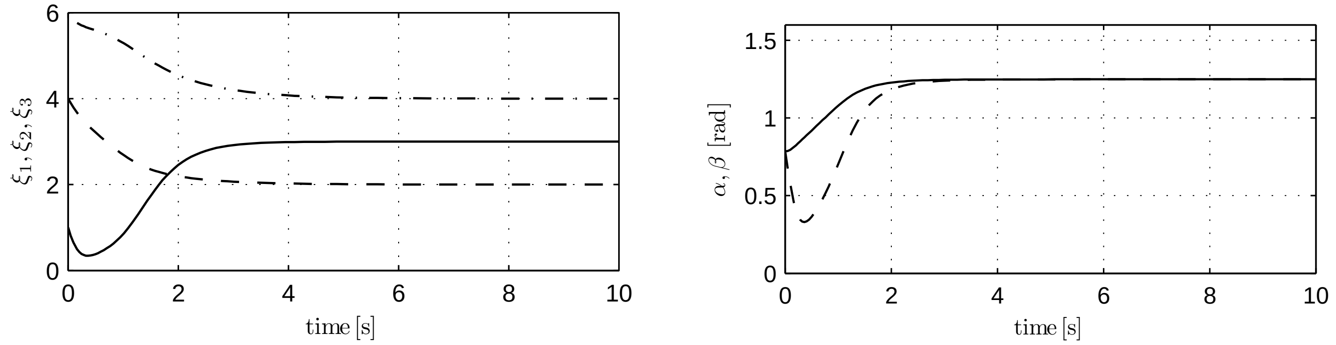

Fig. 7. Results of simulation Sim A3 for $m = 1$

a) Coordinates: ξ_1 (–), ξ_2 (-.), ξ_3 (- -) b) Angles: α (–), β (-.)

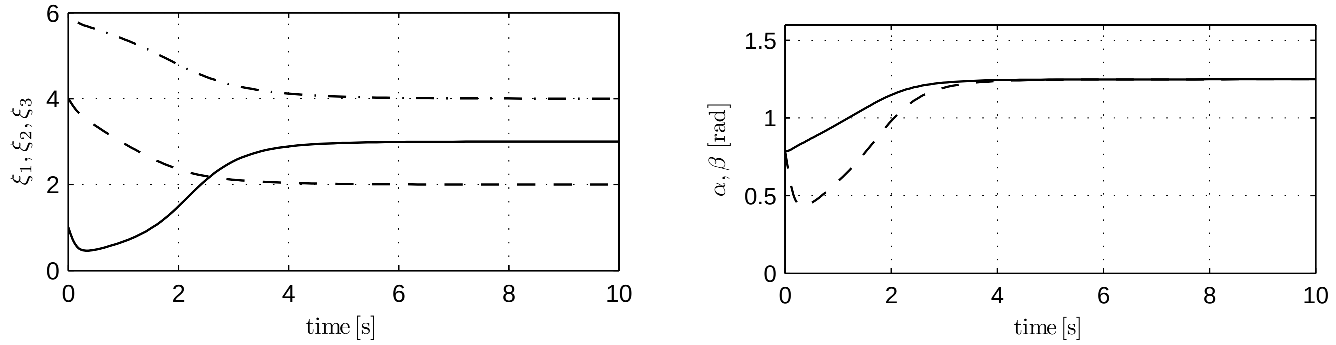

Fig. 8. Results of simulation Sim A3 for $m = 9$

The conditions of simulation Sim B3 correspond to the ones used in the simulation Sim B1. The results of simulations are illustrated for $c = 0.05$ and $c = 1$ in Figs. 9 and 10, respectively. Referring to relationship (46) it can be easily found that for $c = 0.05$ and given gains k_1 and k_2 highly oscillatory behavior appears (at least locally). It can be ob-

Unauthenticated | 89.67.242.59
Download Date | 5/19/13 8:28 PM

served in Fig. 9 that errors converge to zero in an oscillatory manner. Considering Fig. 9c a significant increase of the control input is presented at about 5^{th} sec. when β becomes near $\pi/2$ (i.e. near $\partial\Omega$) as a result of an overshoot – cf. Fig. 9d. In spite of it the control inputs are bounded during the converge stage.

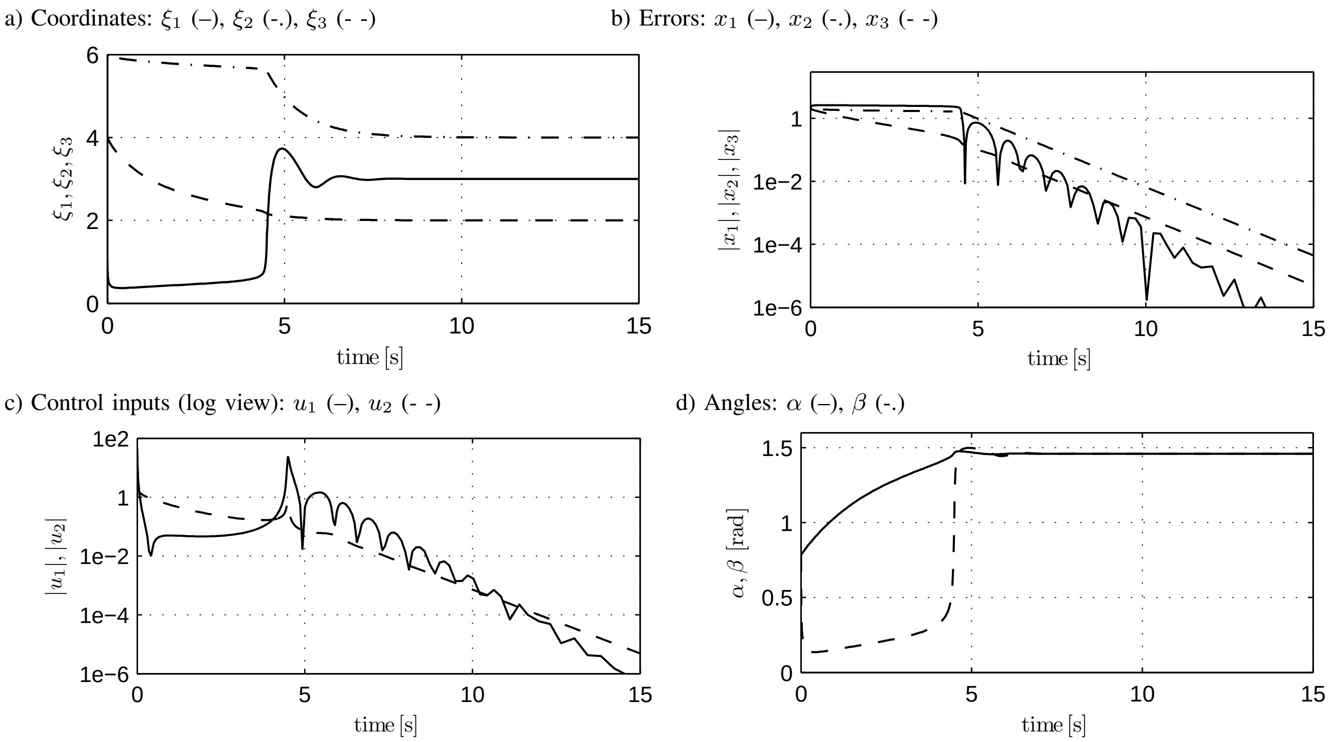

Fig. 9. Results of simulation Sim B3 for $c = 0.05$

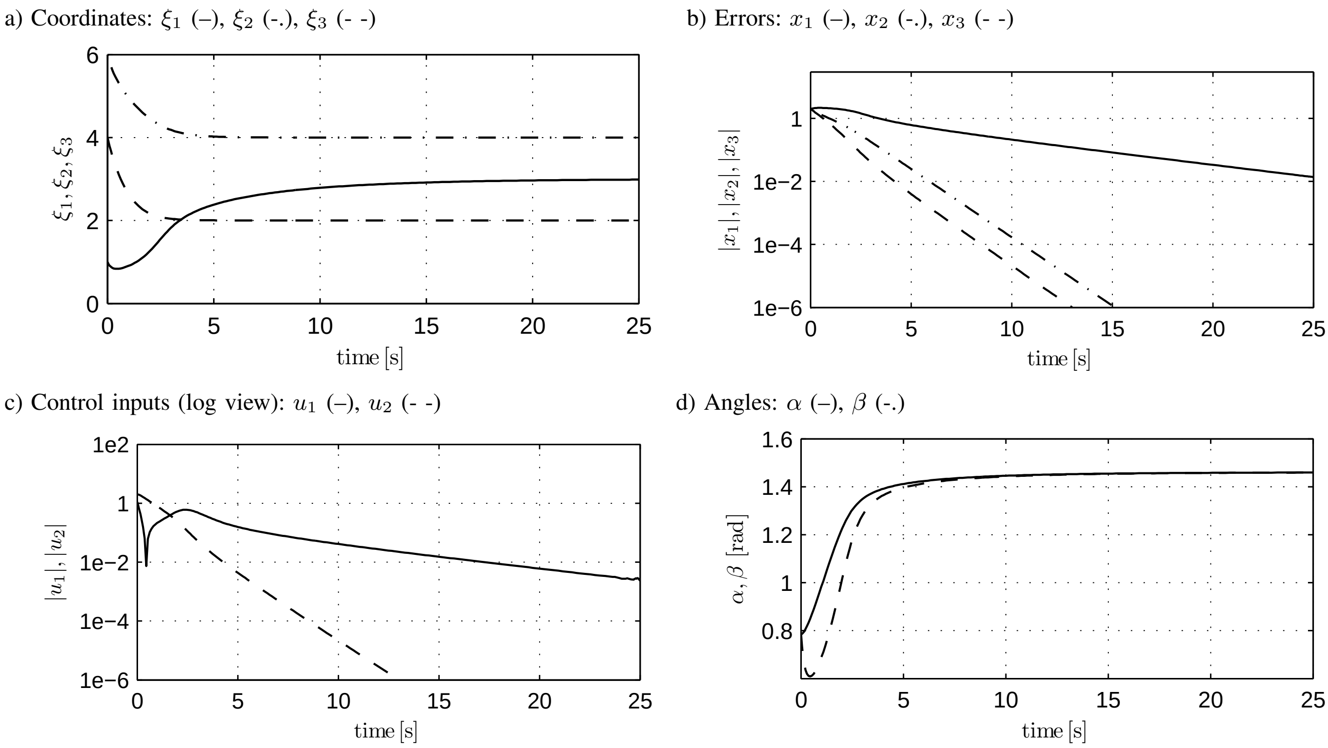

Fig. 10. Results of simulation Sim B3 for $c = 2$

Unauthenticated | 89.67.242.59
Download Date | 5/19/13 8:28 PM

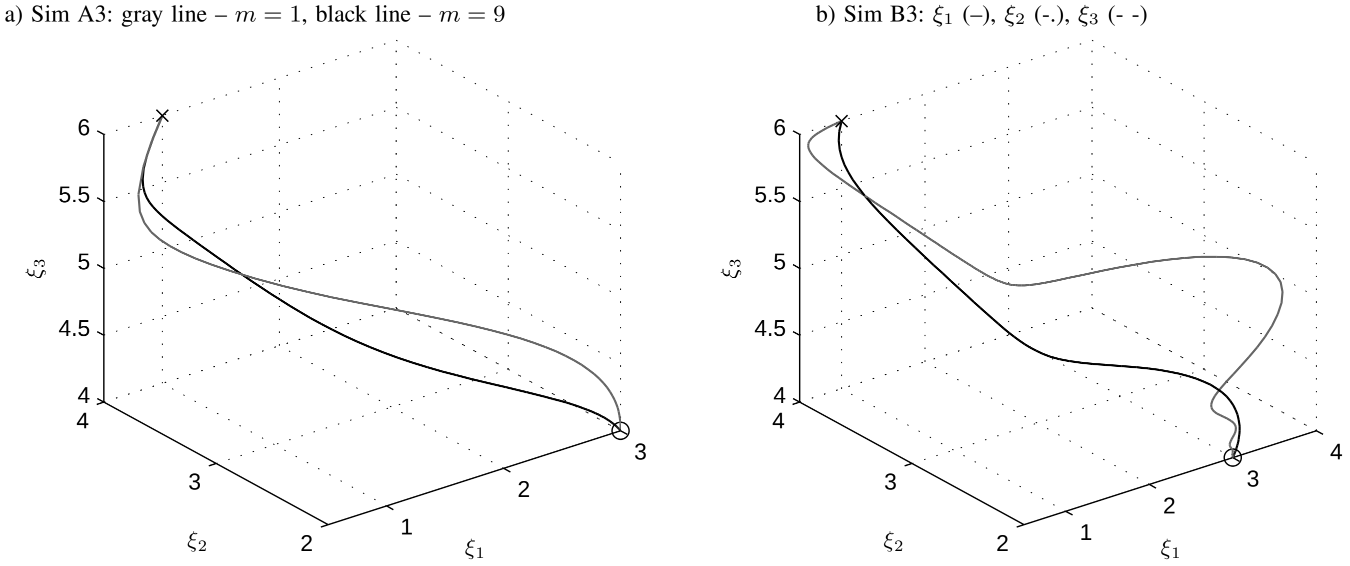

Fig. 11. Path $\boldsymbol{\xi}$ in the coordinate space for simulations Sim A3 and B3

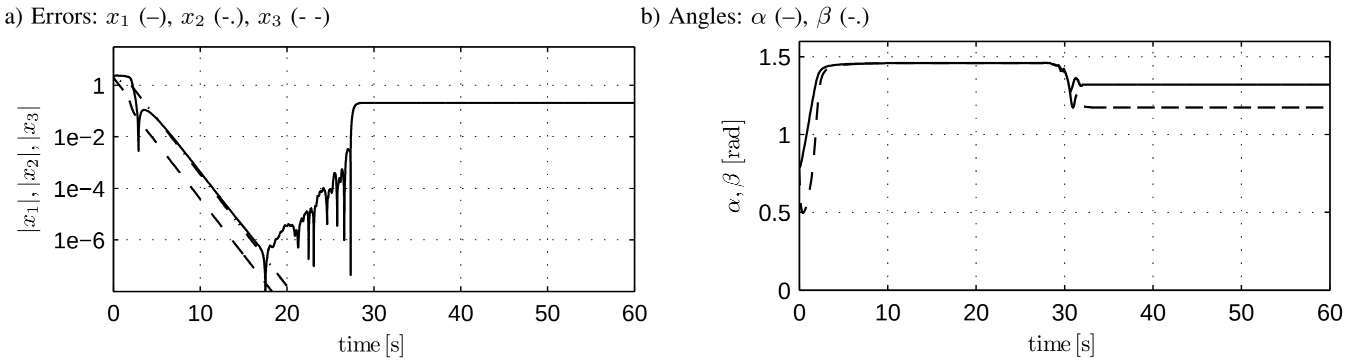

Fig. 12. Results of simulation Sim B1 for longer time horizon (original version of the algorithm)

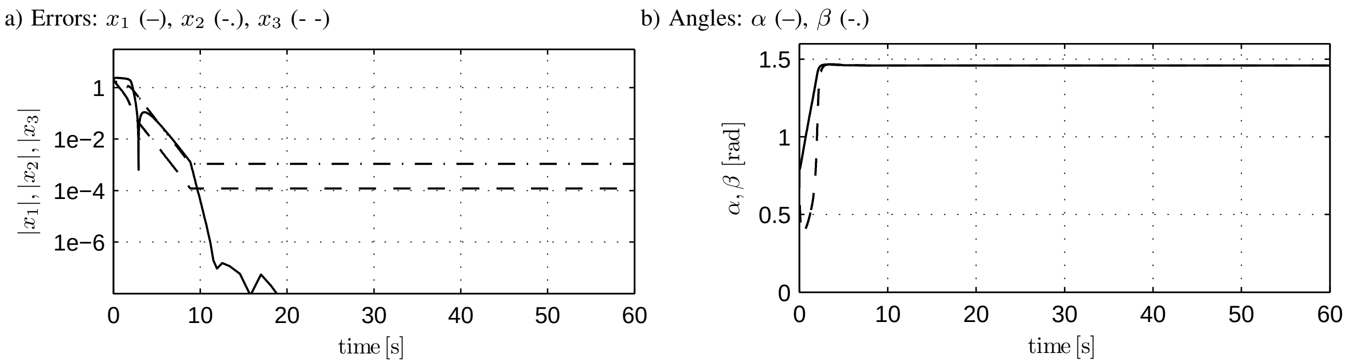

Fig. 13. Results of simulation Sim B1 for longer time horizon (hybrid version of the algorithm)

For higher value of parameter c, namely for $c = 1$, no overshoot and no oscillatory behavior can be recorded – cf. Fig. 10. However, for given k_1 and k_2 the convergence time is increased as a result of higher damping coefficient ζ calculated for the linear approximation of the closed-loop system. Therefore it can be concluded that by increasing the coefficient c the convergent rate of error x_1 becomes worse in comparison with the convergent rate of errors x_2 and x_3. The curves presented in Fig. 11a confirm conclusions formulated regarding the oscillatory behavior of the closed-loop system, namely for $c = 0.05$ the curvature of the path changes significantly (it is especially visible at the neighborhood of

Unauthenticated | 89.67.242.59
Download Date | 5/19/13 8:28 PM

the desired point) while for $c = 1$ the path curvature is reduced.

In the last simulation robustness of the algorithm with respect to numerical representation and its accuracy have been examined. The conditions of the simulation correspond to ones used for Sim B1, however time horizon has been extended to 60 s. According to results illustrated in Figs. 12a and 12b high sensitivity of the controller is observed. Namely, when ρ approaches zero calculation of angle α based on relationship (7) becomes difficult since limitation of numerical representation in Matlab (double precision is used) appears. Hence, for $t > 18$ s destabilization effect is clearly visible which confirms that the closed loop-system is not stable.

The modification of the algorithm based on introduction of the dead zone given in the Proposition 4 gives possibility to overcome this singularity problem. In Fig. 13 the results of simulation assuming $\epsilon = 0.001$ are presented. It can be seen that in this case the behavior of the algorithm is improved by using simple hybrid solution. After 10 s the switching can be recorded and evolution of errors x_2 and x_3 is terminated, while x_1 tends to zero. In the case of additional disturbance (for example in the form of a noise which is added to the coordinates $\boldsymbol{\xi}$) instead of typical switching one can use hysteresis.

6. Conclusions

The algorithm presented in this paper takes advantage of the non-smooth polar coordinate transformation in order to overcome the Brockett's obstruction. By introducing singularity at the origin the system can be controlled using the static-state feedback such that the trajectory error converges to the desired point. The presented solution can be classified as the closed-loop planning (control) algorithm, however, it does not guarantee stability at the desired point. This drawback is clearly a result of discontinuity. In order to overcome this issue simple hybrid solution was considered in the paper.

The algorithm proposed in this paper basically extends the result proposed by Aicardi *et al.* [15] and it summarizes and generalizes the idea of the controllers proposed by Pazderski and others [18, 17]. The simulation results presented here show that the performance of the controller in the terms of oscilatory behavior and the convergence rate is quite good. It was shown that it can be effectively used also for more complicated system with no constant nonholonomy degree, however, the solution may be limited to specified subset of the coordinate space. The indirect Lapunov method used here allows one to obtain the basic principle how to tune the proposed algorithm.

The future work can be devoted to extension of the algorithm to the case of trajectory tracking. Some preliminary results concerning unicycle-like robot are given in [22]. Moreover, it would be interesting to make quantitatively comparison to similar control method based on vector fields orientation (VFO) introduced by Michałek and Kozłowski [23]. The other problem is related to the extension of the presented method to the system evolving in the higher dimensional configuration space. The solution to that problem has been investigated by Aicardi et al. in [24]. Still the open problem is related to the possibility of adaptation of a polar description for other systems with nonholonomic constraints, such as car-like kinematics, vehicles with trailers, higher order chained systems etc.

Appendix

Polar representation – general framework. Consider vector $\boldsymbol{\xi} := [\xi_1 \; \xi_2]^\top \in \mathbb{R}^2$ with $\xi_1, \xi_2 \in \mathbb{R}$. One can use polar representation as follows:

$$\boldsymbol{\xi} := \rho_\varphi \boldsymbol{\psi}(\varphi), \tag{74}$$

where

$$\boldsymbol{\psi}(\varphi) := \begin{bmatrix} \cos\varphi \\ \sin\varphi \end{bmatrix}, \tag{75}$$

$$\rho_\varphi := \|\boldsymbol{\xi}\| \geq 0, \tag{76}$$

and

$$\varphi := \begin{cases} \arg\boldsymbol{\xi} \in (-\pi, \pi] & \text{when } \rho_\varphi > 0 \\ \text{undetermined} & \text{when } \rho_\varphi = 0 \end{cases} \tag{77}$$

with

$$\arg\boldsymbol{\xi} := \operatorname{atan2}(\xi_2, \xi_1). \tag{78}$$

It is important to emphasize that for $\|\boldsymbol{\xi}\| = 0$ function atan2 becomes undetermined and at this point unique value of φ cannot be obtained.

Taking the time derivative of (78) one has

$$\dot{\varphi} = \frac{1}{\xi_1^2 + \xi_2^2}\left(\xi_1\dot{\xi}_2 - \xi_2\dot{\xi}_1\right) = \frac{1}{\rho_\varphi^2}\boldsymbol{\xi}^\top \boldsymbol{J}\dot{\boldsymbol{\xi}} = \frac{1}{\rho_\varphi}\boldsymbol{\psi}^\top(\varphi)\boldsymbol{J}\dot{\boldsymbol{\xi}}, \tag{79}$$

with

$$\boldsymbol{J} := \begin{bmatrix} 0 & 1 \\ -1 & 0 \end{bmatrix} \tag{80}$$

being the skew-symmetric matrix. Assuming that $\dot{\boldsymbol{\xi}} := \rho_\delta \boldsymbol{\psi}(\delta)$, where $\delta := \operatorname{atan2}(\dot{\xi}_2, \; \dot{\xi}_1)$ one obtains

$$\dot{\varphi} = \frac{\rho_\delta}{\rho_\varphi}\boldsymbol{\psi}^\top(\varphi)\boldsymbol{J}\boldsymbol{\psi}(\delta) = \frac{\rho_\delta}{\rho_\varphi}\sin(\delta - \varphi), \tag{81}$$

where $\rho_\delta = \|\dot{\boldsymbol{\xi}}\| \geq 0$.

Linearization of closed-loop dynamics. We assume that the closed loop-dynamics given by Eqs. (30) and (34) is considered at particular point such that $\beta = \beta_0$ and $\alpha = \beta_0$. Considering Taylor expansion the following variables are defined: $\widetilde{\alpha} := \alpha - \beta_0$ and $\widetilde{\beta} := \beta - \beta_0$. The result of linearization of (30) is clear and it can be written as follows:

$$\dot{\widetilde{\alpha}} \approx -k_2\left(\widetilde{\beta} - \widetilde{\alpha}\right). \tag{82}$$

The dynamics described by Eq. (34) is highly nonlinear and more complicated. Hence, particular terms is considered separately in order to facilitate the calculations. To simplify the notation Eq. (34) is rewritten as follows

$$\dot{\beta} = a(\alpha, \beta)\left(\frac{\partial\gamma(\alpha, \beta)}{\partial\beta}\right)^{-1}, \tag{83}$$

Unauthenticated | 89.67.242.59
Download Date | 5/19/13 8:28 PM

where

$$a(\alpha,\beta) = -k_1\gamma(\alpha,\beta) + k_2\sin(\beta-\alpha)\cos^m(\beta-\alpha)\frac{\partial\gamma(\alpha,\beta)}{\partial\alpha} + \frac{k_2}{c}\frac{\sin(\beta-\alpha)}{\gamma(\alpha,\beta)}\gamma(\alpha,\beta_0)\frac{\partial\gamma(\alpha,\beta_0)}{\partial\alpha}\cos^m(\beta-\alpha).$$

Considering linear approximation of $\dot{\beta}$ the following relationship can be obtained

$$\dot{\beta} \approx \left(\frac{\partial a(\alpha,\beta)}{\partial\alpha}\widetilde{\alpha} + \frac{\partial a(\alpha,\beta)}{\partial\beta}\widetilde{\beta}\right)\Big|_{\substack{\alpha=\beta_0\\ \beta=\beta_0}} \kappa_\beta^{-1} - a(\alpha,\beta)|_{\substack{\alpha=\beta_0\\ \beta=\beta_0}}\left(\frac{\partial^2\gamma(\alpha,\beta)}{\partial\beta^2}\widetilde{\beta} + \frac{\partial^2\gamma(\alpha,\beta)}{\partial\alpha\partial\beta}\widetilde{\alpha}\right)_{\substack{\alpha=\beta_0\\ \beta=\beta_0}}\kappa_\beta^{-2} = \left(\frac{\partial a(\alpha,\beta)}{\partial\alpha}\widetilde{\alpha} + \frac{\partial a(\alpha,\beta)}{\partial\beta}\widetilde{\beta}\right)\Big|_{\substack{\alpha=\beta_0\\ \beta=\beta_0}}\kappa_\beta^{-1} \tag{84}$$

with $\kappa_\beta := \frac{\partial\gamma(\alpha,\beta)}{\partial\beta}\Big|_{\substack{\alpha=\beta_0\\ \beta=\beta_0}}$. Taking into account result (84) it follows that it is sufficient to consider terms of function $a(\alpha,\beta)$. The term $\gamma(\alpha,\beta)$ can be expanded as follows:

$$\gamma(\alpha,\beta) \approx \gamma(\beta_0,\beta_0) + \kappa_\alpha\widetilde{\alpha} + \kappa_\beta\widetilde{\beta} = \kappa_\alpha\widetilde{\alpha} + \kappa_\beta\widetilde{\beta}, \tag{85}$$

where $\kappa_\alpha := \frac{\partial\gamma(\alpha,\beta)}{\partial\alpha}\Big|_{\substack{\alpha=\beta_0\\ \beta=\beta_0}}$. Next, considering Taylor linear approximation of $\sin(\beta-\alpha)\cos^m(\beta-\alpha)\frac{\partial\gamma(\alpha,\beta)}{\partial\alpha}$ at considered point one has:

$$\begin{aligned}&\sin(\beta-\alpha)\cos^m(\beta-\alpha)\frac{\partial\gamma(\alpha,\beta)}{\partial\alpha} \approx \\ &\approx \kappa_\alpha\left(\cos(\beta-\alpha)\cos^m(\beta-\alpha) - m\sin^2(\beta-\alpha)\cos^{m-1}(\beta-\alpha)\right)\Big|_{\substack{\alpha=\beta_0\\ \beta=\beta_0}}\left(\widetilde{\beta}-\widetilde{\alpha}\right) \\ &+ \left(\sin(\beta-\alpha)\cos^m(\beta-\alpha)\right)\Big|_{\substack{\alpha=\beta_0\\ \beta=\beta_0}}\left(\frac{\partial^2\gamma(\alpha,\beta)}{\partial\alpha\partial\beta}\widetilde{\beta} + \frac{\partial^2\gamma(\alpha,\beta)}{\partial\alpha^2}\widetilde{\alpha}\right)\Big|_{\substack{\alpha=\beta_0\\ \beta=\beta_0}} = \left(\widetilde{\beta}-\widetilde{\alpha}\right)\kappa_\alpha.\end{aligned} \tag{86}$$

Similarly approximation of $\dfrac{\sin(\beta-\alpha)\gamma(\alpha,\beta_0)}{\gamma(\alpha,\beta)}$ can be calculated as follows:

$$\frac{\sin(\beta-\alpha)}{\gamma(\alpha,\beta)}\gamma(\alpha,\beta_0) \approx -\frac{Z}{\gamma^2(\alpha,\beta)}\Big|_{\substack{\alpha=\beta_0\\ \beta=\beta_0}}\widetilde{\alpha} + \frac{\cos(\beta-\alpha)\gamma(\alpha,\beta_0)\gamma(\alpha,\beta) - \sin(\beta-\alpha)\gamma(\alpha,\beta_0)\kappa_\beta}{\gamma^2(\alpha,\beta)}\Big|_{\substack{\alpha=\beta_0\\ \beta=\beta_0}} \cdot\widetilde{\beta} = (1-\kappa_\gamma\kappa_\beta)\widetilde{\beta} - \widetilde{\alpha} \tag{87}$$

where

$$Z = \cos(\beta-\alpha)\gamma(\alpha,\beta_0)\gamma(\alpha,\beta) + \sin(\beta-\alpha)\frac{\partial\gamma(\alpha,\beta_0)}{\partial\alpha}\gamma(\alpha,\beta) - \sin(\beta-\alpha)\gamma(\alpha,\beta_0)\kappa_\alpha$$

with

$$\kappa_\gamma := \frac{\sin(\beta-\alpha)}{\gamma(\alpha,\beta)}\Big|_{\substack{\alpha=\beta_0\\ \beta=\beta_0}}. \tag{88}$$

Combining (84), (82), (85) and (87) it follows that

$$\begin{aligned}\dot{\beta} &\approx -\frac{k_1}{\kappa_\beta}\left(\kappa_\alpha\widetilde{\alpha} + \kappa_\beta\widetilde{\beta}\right) + \frac{k_2\kappa_\alpha}{\kappa_\beta}\left(\widetilde{\beta}-\widetilde{\alpha}\right) + \frac{k_2\kappa_\alpha}{\kappa_\beta c}\left(\widetilde{\beta}(1-\kappa_\gamma\kappa_\beta) - \widetilde{\alpha}\right) \\ &= -\frac{\kappa_\alpha}{\kappa_\beta}\left(k_1 + k_2 + \frac{k_2}{c}\right)\widetilde{\alpha} + \left(-k_1 + \frac{k_2\kappa_\alpha}{\kappa_\beta}\left(1 + \frac{1-\kappa_\gamma\kappa_\beta}{c}\right)\right)\widetilde{\beta}.\end{aligned} \tag{89}$$

Now we consider definition (88) more thoroughly in order to find some relationships between κ_γ, κ_α and κ_β. Assuming that $\exists t_f > 0$ such that $\alpha(t_f) = \beta_0$ and $\beta(t_f) = \beta_0$ one can rewrite (89) as follows

$$\kappa_\gamma := \lim_{t\to t_f}\frac{\sin(\beta(t)-\alpha(t))}{\gamma(\alpha(t),\beta(t))}. \tag{90}$$

Applying de l'Hospital rule yields in

$$\kappa_\gamma = \lim_{t\to t_f}\frac{\cos(\beta(t)-\alpha(t))\left(\dot{\beta}-\dot{\alpha}\right)}{\dfrac{\partial\gamma}{\partial\alpha}\dot{\alpha} + \dfrac{\partial\gamma}{\partial\beta}\dot{\beta}} = \frac{\dot{\beta}(t_f) - \dot{\alpha}(t_f)}{\kappa_\alpha\dot{\alpha}(t_f) + \kappa_\beta\dot{\beta}(t_f)}. \tag{91}$$

Then in order to find the limit of (91) for any $\dot{\alpha}$ and $\dot{\beta}$ partial derivatives of γ should satisfy: $\kappa_\alpha = -\kappa_\beta$. Consequently, it gives

$$\kappa_\gamma = \frac{1}{\kappa_\beta} \tag{92}$$

which allows one to simplify expression (89) as follows

$$\dot{\beta} \approx \left(k_1 + k_2 + \frac{k_2}{c}\right)\widetilde{\alpha} + (-k_1 - k_2)\widetilde{\beta}. \tag{93}$$

Definition of modulo operators for angle variables. Describing rotation on the plane one can use rotation matrix $\boldsymbol{R} \in \mathrm{SE}(2)$ which can be parametrized by angle $\varphi \in \mathbb{S}^1$. Hence, a rotation about angle φ can be described as follows: $\boldsymbol{R}|_\varphi = \boldsymbol{R}(\varphi) = \left[\begin{smallmatrix}\cos\varphi & -\sin\varphi\\ \sin\varphi & \cos\varphi\end{smallmatrix}\right]$. It turns out that every distinguished rotation on the plane can be realized assuming the following parametrization of angle: $\varphi \in (-\pi,\pi]$. The given parametrization should be taken into account more thoroughly with respect to superposition of rotations. Considering two rotations about angles $\varphi_1 \in (-\pi,\pi]$ and $\varphi_2 \in (-\pi,\pi]$ one has: $\boldsymbol{R}|_{\varphi_1}\boldsymbol{R}|_{\varphi_2} = \boldsymbol{R}(\varphi) = \boldsymbol{R}(\varphi_1+\varphi_2)$. As a result of periodicity of sine and cosine functions the resultant angle of rotation can be specified in the range $(-\pi,\pi]$. However, using typical algebraic addition or subtraction $\varphi_1 \pm \varphi_2$ may go out from the assumed range. Instead of it one can use modulo

Unauthenticated | 89.67.242.59
Download Date | 5/19/13 8:28 PM

operators $\oplus$ and $\ominus$ in order to interpret the results properly. These operators are defined as follows:

$$\forall\ \varphi_1, \varphi_2 \in (-\pi, \pi]\ \ \varphi_1 \oplus \varphi_2 := \begin{cases} \varphi_1 + \varphi_2 & \text{for } \varphi_1 + \varphi_2 \in (-\pi, \pi] \\ \varphi_1 + \varphi_2 + 2\pi & \text{for } \varphi_1 + \varphi_2 < -\pi \\ \varphi_1 + \varphi_2 - 2\pi & \text{for } \varphi_1 + \varphi_2 > \pi \end{cases} \tag{94}$$

and

$$\forall\ \varphi_1, \varphi_2 \in (-\pi, \pi]\ \ \varphi_1 \ominus \varphi_2 := \begin{cases} \varphi_1 - \varphi_2 & \text{for } \varphi_1 - \varphi_2 \in (-\pi, \pi] \\ \varphi_1 - \varphi_2 + 2\pi & \text{for } \varphi_1 - \varphi_2 < -\pi \\ \varphi_1 - \varphi_2 - 2\pi & \text{for } \varphi_1 - \varphi_2 > \pi \end{cases}. \tag{95}$$

Acknowledgements. This work was supported under the university grant No. 507/93/193/12 DS-MK and the Polish Ministry of Science and Higher Education grant No. N N514 406236.

REFERENCES

[1] R.W. Brockett, Asymptotic stability and feedback stabilization, In *Differential Geometric Control Theory*, eds. R.W. Brockett, R.S. Millman, and H.J. Sussmann, pp. 181–191, Birkhäuser, Boston, 1983.

[2] C. Samson, "Velocity and torque feedback control of a nonholonomic cart", *Advanced Robot Control*, eds. C. Canudas de Witpages, pp. 125–151, Birkhauser, Boston, 1991.

[3] J.B. Pomet, "Explicit design of time varying stabilization control laws for a class of controllable systems without drifts", *Systems and Control Letters* 48, 147–158 (1992).

[4] C. Canudas de Wit and O.J. Sørdalen, "Exponential stabilization of mobile robots with nonholonomic constraints", *IEEE Trans. Automatic Control* 37, 1791–1797 (1992).

[5] A. Astolfi, "Exponential stabilization of a wheeled mobile robot via discontinuous control", *Nonlinear Control System Design Symposium* 1, 741–746 (1995).

[6] R.T. M'Closkey and R.M. Murray, "Exponential stabilization of driftless nonlinear control systems using homogeneous feedback", *IEEE Trans. on Automatic Control* 42, 614–628 (1995).

[7] P. Morin and C. Samson, "Trajectory tracking for nonholonomic vehicles: overview and case study", *Proc. 4th Int. Workshop on Robot Motion and Control* 1, 139–153 (2004).

[8] D.A. Lizárraga, P. Morin, and C. Samson, "Non-robustness of continuous homogeneous stabilizers for affine control systems", *Proc. of Conf. on Decision and Control* 1, 855–860 (1999).

[9] P. Morin and C. Samson, "Practical stabilization of driftless systems on Lie groups: the transverse function approach", *IEEE Trans. on Automatic Control* 48 (9), 1496–1508 (2003).

[10] I. Dulęba, "Impact of control representations on efficiency of local nonholonomic motion planning", *Bull. Pol. Ac.: Tech.* 59 (2), 213–218 (2011).

[11] G. Lafferriere and H.J. Sussmann, "A differential geometric approach to motion planning", in *Nonholonomic Motion Planning*, pp. 235–270, Kluwer, London, 1993.

[12] R. Murray and S.S. Sastry, "Nonholonomic motion planning: Steering using sinusoids", *IEEE Trans. on Automatic Control* 38, 700–716 (1993).

[13] M. Fliess, J.L. Lévine, P. Martin, and P. Rouchon, "Flatness and defect of non-linear systems: introductory theory and examples", *Int. J. Control* 61 (6), 1327–1361 (1995).

[14] I. Dulęba and J.Z. Sąsiadek, "Nonholonomic motion planning based on Newton algorithm with energy optimization", *IEEE Trans. on Control Systems Technology* 11 (3), 355–363 (2003).

[15] M. Aicardi, G. Casalino, A. Bicchi, and A. Balestrino, "Closed loop steering of unicycle-like vehicles via Lyapunov techniques", *IEEE Robotics and Automation Magazine* 2, 27–35 (1995).

[16] G. Oriolo, A. De Luca, and M. Venditteli, "WMR control via dynamic feedback linearization: design, implementation and experimental validation", *IEEE Trans. on Control System Technology* 1, 835–852 (2002).

[17] D. Pazderski, K. Kozłowski, and K. Krysiak, "Nonsmooth stabilizer for three link nonholonomic manipulator using polar-like coordinate representation", in *Robot Motion and Control*, vol. 396, pp. 35–44, Springer-Verlag, Berlin, 2009.

[18] D. Pazderski, K. Kozłowski, and J.K. Tar, "Discontinuous stabilizer of the first order chained system using polar-like coordinates transformation", *Proc. Eur. Control Conf.* 1, 2751–2756 (2009).

[19] J.-J. Slotine and W. Li, *Applied Nonlinear Control*, Prentice Hall, New York, 1990.

[20] D. Pazderski, B. Krysiak, and K. Kozłowski, "A comparison study of discontinuous control algorithms for three-link nonholonomic manipulator", in *Robot Motion and Control*, vol. 422, pp. 377–389, Springer-Verlag, Berlin, 2012.

[21] J.P. Laumond, S. Sekhavat, and F. Lamiraux, "Guidelines in nonholonomic motion planning for mobile robots", in *Robot Motion Planning and Control*, vol. 229, pp. 1–54, Springer-Verlag, Berlin, 1998.

[22] D. Pazderski, P. Szulczyński, and K. Kozłowski, "Kinematic tracking controller for unicycle mobile robbot based on polar-like representation and Lyapunov analysis", in *Robot Motion and Control*, vol. 396, pp. 45–56, Springer-Verlag, Berlin, 2009.

[23] M. Michałek and K. Kozłowski, "Vector-field-orientation feedback control method for a differentially driven vehicle", *IEEE Trans. on Control Systems Technology* 18 (1), 45–65 (2010).

[24] M. Aicardi, G. Cannata, G. Casalino, and G. Indiveri, "Guidance of 3D underwater non-holonomic vehicle via projection on holonomic solutions", *8th Int. Symp. on Robotics with Applications* 1, CD-ROM (2000).

Unauthenticated | 89.67.242.59
Download Date | 5/19/13 8:28 PM